Supporting information for:

Crystal structures of *Acetobacter aceti* succinyl-coenzyme A (CoA):acetate CoA-transferase (AarC) reveal specificity determinants and illustrate the mechanism used by class I CoA-transferases

Elwood A. Mullins[†,‡] and T. Joseph Kappock[*,†]

Department of Biochemistry, Purdue University, West Lafayette, Indiana 47907-2063, United States

E-mail: kappock@purdue.edu

Phone: 765-494-8383. Fax: 765-494-1897

[*]To whom correspondence should be addressed

[†]Department of Biochemistry, Purdue University, West Lafayette, Indiana 47907

[‡]Department of Chemistry, Washington University, St. Louis, Missouri 63130

Supporting Experimental Methods

Purification of AarCH6 and AarCH6 Mutants. *Escherichia coli* C41(DE3) cells transformed with pJK385 were propagated on Luria-Bertani (LB)[1] medium containing 100 $\mathrm{mg\,L^{-1}}$ ampicillin and 70 $\mathrm{mg\,L^{-1}}$ kanamycin (LB/Amp/Kan). Production cultures (1 L LB/Amp/Kan) were inoculated with overnight cultures at a 1:500 dilution and grown at 37 °C to mid-log phase ($\mathrm{OD}_{600} = 0.6$). Production of recombinant AarCH6 was then induced by addition of isopropyl-β-D-1-thiogalactopyranoside to 0.4 mM. Cultures were grown at 15 °C an additional 16 h, harvested by centrifugation, and either used immediately or stored at −80 °C. All subsequent steps were performed at 4 °C.

Cells (typically $5-10$ g) were resuspended in 5 $\mathrm{mL\,g^{-1}}$ of buffer TK [50 mM Tris · HCl (pH 8.0) and 100 mM potassium chloride] and disrupted by sonication. Lysate was cleared by centrifugation at 30000*g* for 30 min, addition of streptomycin to 1% (w/v) from a 10% (w/v) stock, incubation for 15 min, and additional centrifugation at 30000*g* for 30 min. Solid ammonium sulfate was then added to the cleared lysate to 35% saturation (208 $\mathrm{g\,L^{-1}}$) with stirring over 30 min. After stirring an additional 30 min, solids were removed by centrifugation at 30000*g* for 10 min. Solid ammonium sulfate was then added to the supernatant to 75% saturation (275 $\mathrm{g\,L^{-1}}$) with stirring over 30 min. After stirring an additional 30 min, solids were collected by centrifugation at 30000*g* for 10 min, dissolved in a minimal volume of buffer TK, and applied to a Ni^{2+}-charged nitrilotriacetic acid (NiNTA) agarose column (1.5 cm × 2.5 cm, 4.4 mL) equilibrated in buffer TN [50 mM Tris · HCl (pH 8.0) and 300 mM sodium chloride]. The column was rinsed with 10 column volumes (CV) of buffer TN containing 10 mM imidazole and then developed in a linear gradient of imidazole in buffer TN (10 → 500 mM, 40 mL × 40 mL). Fractions containing AarCH6 were identified by sodium dodecyl sulfate polyacrylamide gel electrophoresis (SDS-PAGE), pooled, and concentrated to > 5 $\mathrm{mg\,mL^{-1}}$ by ultrafiltration (Amicon Ultra-15, 30000 molecular weight cut-off

[1] Additional abbreviations: CV, column volumes; DEAE, diethylaminoethyl; DTNB, 5,5′-dithiobis(2-nitrobenzoic acid); LB, Luria-Bertani medium; LCC, longest linear carbon chain; MWCO, molecular weight cut-off; NA, not applicable; NiNTA, Ni^{2+}-charged nitrilotriacetic acid agarose; NJ, neighbor-joining; Rms, root-mean-square; SDS-PAGE, sodium dodecyl sulfate polyacrylamide gel electrophoresis; SBSA, structure-based sequence alignment; T_m, melting temperature.

[MWCO]). A portion of the purified AarCH6 was exchanged into buffer TK by several cycles of dilution and reconcentration. The remaining purified AarCH6 (10 mg) was applied to a Sephadex G200 column (2.5 cm × 28.0 cm, 140 mL) equilibrated and then developed in buffer TK. Fractions containing AarCH6 were identified by SDS-PAGE, pooled, and concentrated by ultrafiltration as described above. Single-use aliquots were flash-frozen and stored at −80 °C.

AarCH6 mutants were isolated using the procedure described above, except for AarCH6-E294A, which was isolated from *E. coli* C41(DE3)/pJK513 grown in LB medium containing 100 $\mathrm{mg\,L^{-1}}$ ampicillin (LB/Amp). The G200 gel-filtration step was omitted for all mutants.

Purification of AarC. *E. coli* C41(DE3) cells transformed with pJK357 were propagated on LB/Amp. The procedure described for AarCH6 was followed up to the streptomycin step, except that cells were resuspended in buffer PK6 [50 mM potassium phosphate (pH 6.0) and 100 mM potassium chloride]. The streptomycin supernatant was adjusted to 43% saturation by the addition of solid ammonium sulfate (263 $\mathrm{g\,L^{-1}}$) with stirring over 30 min. After stirring an additional 30 min, solids were removed by centrifugation at 30 000*g* for 10 min and the supernatant was adjusted to 68% saturation by the addition of solid ammonium sulfate (167 $\mathrm{g\,L^{-1}}$) with stirring over 30 min. After stirring an additional 30 min, solids were collected by centrifugation at 30 000*g* for 10 min, dissolved in a minimal volume of buffer P7 [20 mM potassium phosphate (pH 7.0)], and applied to a Sephadex G25 column (2.5 cm × 40 cm, 200 mL). The column was developed with several CV of buffer P7. Fractions with low conductivity and high A_{280} were pooled, concentrated by ultrafiltration as described above, and applied to a diethylaminoethyl (DEAE) Sepharose CL-6B column (2.5 cm × 8.0 cm, 39 mL) equilibrated in buffer P7. The column was washed with one CV of buffer P7 and then developed in a linear gradient of potassium chloride in buffer P7 (0 → 1.2 M, 400 mL × 400 mL). Fractions containing AarC were identified by SDS-PAGE, pooled, concentrated by ultrafiltration as described above, exchanged into buffer MMK [50 mM Mes (pH 6.2), 5 mM magnesium chloride, and 20 mM potassium chloride] by several cycles of dilution and reconcentration, and applied to a Cibacron Blue 3GA agarose column (2.5 cm × 12.5

cm, 61 mL) equilibrated in buffer MMK. The column was washed with one CV of buffer MMK and then developed in a linear gradient of potassium chloride in buffer MMK (0.02 → 1.2 M, 350 mL × 350 mL). Fractions containing AarC were identified by SDS-PAGE, pooled, concentrated by ultrafiltration as described above, exchanged into buffer PK8 [50 mM potassium phosphate (pH 8.0) and 100 mM potassium chloride] by several cycles of dilution and reconcentration. Single-use aliquots were flash-frozen and stored at −80 °C.

Circular Dichroism (CD) Measurements. Thermal denaturation of AarC and AarCH6 was monitored using a Chirascan spectropolarimeter (Applied Photophysics). AarC or AarCH6 (19 $\mu g\,mL^{-1}$, 0.34 μM) was equilibrated at 20 °C for 30 min in a 10 mm pathlength quartz cuvette containing 50 mM potassium phosphate (pH 3.5 – 8.5) and 100 mM potassium chloride. Replicate far-UV spectra (3 scans, 200 – 260 nm, 1 nm bandwidth, 1 nm step, 1 s $step^{-1}$) were recorded at 20 °C. (Each sample spectrum was corrected by subtracting a buffer-only spectrum.) The sample was then heated from 20 – 90 °C at a continuous rate of 0.5 $°C\,min^{-1}$. Ellipticity was monitored at 222 nm (1 nm bandwidth) by averaging the signal for 12 s at each 0.5 °C step. The solution temperature was directly measured using a probe inserted through the cuvette stopper. Melting profiles were fit to a double-sigmoid equation using Pro-Data Viewer (Applied Photophysics) and the steepest point of each profile was taken as the melting temperature (T_m).

Electrospray-Ionization Time-of-Flight Mass Spectrometry (ESI-TOF-MS) Protein masses (Table S3) were determined by ESI-TOF-MS by the staff of the Washington University Mass Spectrometry Resource.

Sequence and Structure Comparisons. The DALI server[S1] was used to identify structures resembling AarCH6 · CoA · citrate (PDB id 4eu7). A group of ten representative class I CoA-transferase structures was selected for further analysis (Supporting Information, Table S17). Dimeric structures were extracted from larger asymmetric units or prepared by the addition of symmetry-related chains using PDBEditor.[S2] Some class I CoA-transferases consist of two polypeptides, α

and β, that correspond to the N- and C-terminal domains of AarC and other single-subunit CoA-transferases.[S3] The α subunit of *Acidaminococcus fermentans* GCT (UniProt/PDB ids Q59111/1poi) was used to place one $\alpha\beta$ protomer, which corresponds to a single AarC subunit.

Structure-based sequence alignments (SBSAs) containing three, six, or all ten structures were assembled using the MatchMaker and Match→Align components of the Chimera package[S4] and manually edited using JalView.[S5] SBSA3 contained PDB ids 4eu7, 2g39, and 2nvv (SCACT group). SBSA6 added PDB ids 2oas, 3eh7, and 3qdq (4HBCT group) to SBSA3.

The AarC sequence was aligned using CD-Search[S6] to a group of putative succinyl-CoA transferases (TIGR03458, 27 Sep 2007 version). The curated representative set of aligned sequences and three AarC homologues from other AAB were added to the SBSA3 alignment to give a set of 26 aligned sequences. All sequences were truncated at the ends of the TIGR03458 HMM model (length 493).

MEGA5[S7] was used to generate a protein distance matrix (Jones-Thornton-Taylor amino acid substitution model), to assemble neighbor-joining (NJ) trees with 1000 bootstrap replicates, and to compute consensus trees. Identification of residues differentially conserved among aligned subgroups was performed using JalView and the Multi-Harmony server.[S8]

Supporting Tables

Table S1: Oligodeoxynucleotides (ODNs) used in this study.[a]

ODN	Sequence ($5' \rightarrow 3'$)	AarCH6-X	plasmid
2079	GCACGAATGACCGGGACGAGAATGCCCCGTTTGCCGC	R228E	pJK512
2080	GCGGCAAACGGGGCATTCTCGTCCCGGTCATTCGTGC	R228E	pJK512
2081	CTGGTGGGCTATAGTGCGGTGATTCAGGATGGC	E294A	pJK513
2082	GCCATCCTGAATCACCGCACTATAGCCCACCAG	E294A	pJK513
2083	GATTTTTGTAACCGCGCAGGGGCTGGCGG	E435A	pJK514
2084	CCGCCAGCCCCTGCGCGGTTACAAAAATC	E435A	pJK514
2093	CAGATTTTTGTAACCCAGCAGGGGCTGGCG	E435Q	pJK516
2094	CGCCAGCCCCTGCTGGGTTACAAAAATCTG	E435Q	pJK516
2095	CAGATTTTTGTAACCGATCAGGGGCTGGCGGATC	E435D	pJK517
2096	GATCCGCCAGCCCCTGATCGGTTACAAAAATCTG	E435D	pJK517
2101	AGCAGGATGTCAGCGCCAGCCCCGGCATTA	N347A	pJK524
2102	TAATGCCGGGGCTGGCGCTGACATCCTGCT	N347A	pJK524
2176	CAGCTGAGGGCCTGTGGCTGCGCCCGTAATCAG	S71A	pJK564
2177	CTGATTACGGGCGCAGCCACAGGCCCTCAGCTG	S71A	pJK564

[a] Underlined bases indicate mutated positions.

Table S2: Isolation of AarC.

operation	protein (mg)	activity (units)	specific activity (s^{-1})[a]	yield (%)
streptomycin	550	3200	5.9	100
43 – 68% $(NH_4)_2SO_4$	260	2600	10	81
G25	200	2400	12	75
DEAE	33	2000	60	63
Cibacron Blue 3GA	5.7	400	71	13

[a] Computed assuming one active site per 54.8 kDa subunit. One unit per mg corresponds to a specific activity of 0.91 s^{-1}.

Table S3: ESI-TOF-MS data for AarC and AarCH6 forms.

Enzyme form	Expected (Da)[a]	Observed (Da)	Difference (Da)
AarC	54 695	54 695	0
AarCH6[b]	55 847	55 847	0
AarCH6-S71A	55 831	55 831	0
AarCH6-R228E	55 821	55 820	1
AarCH6-E294A	55 789	55 789	0
AarCH6-N347A	55 804	55 804	0
AarCH6-E435D	55 833	55 833	0

[a] Computed assuming Met1 is missing.
[b] From Ref. S9.

Table S4: Kinetic characterization of alternate carboxylate substrates for AarCH6.[a]

LCC[b]	acid	k_{cat} (s^{-1})	K_m (mM)	K_i (mM)	k_{cat}/K_m (M^{-1} s^{-1})
C1	formate	1.9	75	NA[c]	26
C2[d]	acetate[e,f]	280	70	1500	4000
C3[g]	propionate	65	240	1600	270
	propionate[e]	65	310	1400	210
C4[h]	acetoacetate[e,f]	37	130	NA	280
	fumarate	0.89	5.4	NA	160
	D-malate (5.7 min)[i]	12	55	NA	220
	L-malate (4.1 min)[j]	0.74	19	NA	39
	L-malate (5.7 min)[j]	0.8	20	NA	40
	DL-methylsuccinate[k]	0.46	58	NA	7.9
	oxaloacetate	0.083	9.4	NA	8.8
	succinate[f]	71	0.9	NA	79 000
C5[l]	glutarate	0.27	290	NA	0.93

[a] Measured using modified LCR assays containing 1 mM acetyl-CoA as described in the main text, except as noted. Saturation curves were performed in duplicate. The limit of detection corresponds to $k_{cat} \leq 0.009$ s^{-1} (~ 0.01 unit mg^{-1}).
[b] LCC, longest linear carbon chain.
[c] NA, not applicable.
[d] C2 with no activity: glycolate, glyoxylate, oxalate, and trifluoroacetate.
[e] Assays contained 50 mM potassium phosphate (pH 8.0), 100 mM potassium chloride, 0.2 mM succinyl-CoA, varying concentrations of carboxylate substrate, and 5 – 50 ng AarCH6.
[f] From Ref. S9.
[g] C3 with no activity: DL-lactate, L-lactate, malonate, and pyruvate.
[h] C4 with no activity: butyrate, maleate, D-tartrate, and L-tartrate.
[i] Peak retention time is given for the major peak of the two product peaks detected, which are presumed to be the regioisomers 2(*R*)- and 3(*R*)-hydroxysuccinyl-CoA. The minor peak, which is presumed to result from the other regioisomer, was observed at 4.1 min.
[j] Peak retention times are given for the two products detected, which are presumed to be the regioisomers 2(*S*)- and 3(*S*)-hydroxysuccinyl-CoA.
[k] Determined in the presence of a small amount of contaminating succinate. The two acyl-CoA product peaks were resolved.
[l] C5 with no activity: α-ketoglutarate, citrate, and DL-isocitrate.

Table S5: Substrate probability values used to compute I and J.[a]

substrate	substrate probability p_i[b]
formate	3.1×10^{-4}
acetate	4.8×10^{-2}
propionate	3.2×10^{-3}
acetoacetate	3.3×10^{-3}
fumarate	1.9×10^{-3}
D-malate	2.6×10^{-3}
L-malate[b]	9.4×10^{-4}
DL-methylsuccinate	9.4×10^{-5}
oxaloacetate	1.1×10^{-4}
succinate	0.94
glutarate	1.1×10^{-5}

[a] Substrate promiscuity index I and weighted substrate promiscuity index J are defined in Ref. S10.

[b] Values computed for N substrates i using

$$p_i = \frac{(k_{\mathrm{cat}}/K_{\mathrm{m}})_i}{\sum_{i=1}^{N} (k_{\mathrm{cat}}/K_{\mathrm{m}})_i} \tag{S1}$$

[c] The sum of the $k_{\mathrm{cat}}/K_{\mathrm{m}}$ values obtained for the two products formed from L-malate was considered for this analysis (Table S4).

Table S6: Substrate structure keyset values.

substrate	keyset[a]
formate	1110000000 0000100001 0000000000 0000000000 0000001010 0000000000 0000000000 0000000000 0000000000 00
acetate	1110000000 0000100001 0000000000 0000000010 0000001010 0000000000 0000000000 0000000000 0000000000 00
propionate	1110000000 0000100001 0000000000 0000000011 0000001010 0000000000 0000000000 0000000000 0000000000 00
acetoacetate	1110000000 0100100001 0000000000 0000000011 0000001110 0000001000 0000000000 0000000000 0000000000 00
fumarate	1110000000 0100100001 1000000000 0000000011 0000001111 0000000000 0000000000 0000000000 0000110000 00
D-malate	1110000000 0100100001 0000000000 0000000011 0000001111 0000100000 0000000000 0000000000 0000000000 00
L-malate	1110000000 0100100001 0000000000 0000000011 0000001111 0000100000 0000000000 0000000000 0000000000 00
DL-methylsuccinate	1110000000 0100100001 0000000000 0000000011 0000001111 0000000000 0000000000 0000000000 0000000000 00
oxaloacetate	1110000000 0100100001 0000000000 0000000011 0000001111 0000001000 0000000000 0000000000 0000000000 00
succinate	1110000000 0100100001 0000000000 0000000011 0000001111 0000000000 0000000000 0000000000 0000000000 00
glutarate	1110000000 0100100001 0000000000 0000000011 1000001111 0000000000 0000000000 0000000000 0000000000 00

[a] Each bit is a score in the 92-part keyset developed in Ref. S10.

Table S7: Tanimoto distance matrices for the screened substrate set.[a]

	formate	acetate	prop.	aceto.	fumar.	D-mal.	L-mal.	DL-ms.	OAA	succ.	glut.
formate	0	0.205	0.364	0.682	0.873	0.755	0.755	0.682	0.755	0.682	0.755
acetate	0.125	0	0.182	0.545	0.764	0.629	0.629	0.545	0.629	0.545	0.629
propionate	0.222	0.111	0	0.503	0.716	0.584	0.584	0.503	0.584	0.503	0.584
acetoacetate	0.417	0.333	0.308	0	0.511	0.351	0.351	0.252	0.126	0.252	0.351
fumarate	0.533	0.467	0.438	0.313	0	0.409	0.409	0.327	0.409	0.327	0.409
D-malate	0.462	0.385	0.357	0.214	0.250	0	0.000	0.126	0.234	0.126	0.234
L-malate	0.462	0.385	0.357	0.214	0.250	0.000	0	0.126	0.234	0.126	0.234
DL-methylsucc.	0.417	0.333	0.308	0.154	0.200	0.077	0.077	0	0.126	0.000	0.126
oxaloacetate	0.462	0.385	0.357	0.077	0.250	0.143	0.143	0.077	0	0.126	0.234
succinate	0.417	0.333	0.308	0.154	0.200	0.077	0.077	0.000	0.077	0	0.126
glutarate	0.462	0.385	0.357	0.214	0.250	0.143	0.143	0.077	0.143	0.077	0

[a] Values below the diagonal are Tanimoto distances. Values above the diagonal are normalized Tanimoto distances, computed as described.[S10]

Table S8: Crystallographic data collection statistics for AarCH6.[a]

Ligands PDB id	(none)[b] 4eu3	CoA 4eu4	CoA 4eu5	CoA, acetate[c] 4eu6	CoA, citrate 4eu7
Beamline	21-ID-F	21-ID-G	23-ID-D	21-ID-F	21-ID-G
Wavelength (Å)	0.97872	0.97856	1.0331	0.97872	0.97856
Space group	$P2_12_12_1$	$P6_222$	$P2_12_12_1$	$P2_12_12_1$	$P2_12_12_1$
Cell dimen. (Å)	$a = 67.5, b = 110.3,$ $c = 119.8$ $\alpha = \beta = \gamma = 90°$	$a = b = 150.2,$ $c = 290.4$ $\alpha = \beta = 90°, \gamma = 120°$	$a = 67.6, b = 110.6,$ $c = 119.5$ $\alpha = \beta = \gamma = 90°$	$a = 67.2, b = 110.4,$ $c = 119.8$ $\alpha = \beta = \gamma = 90°$	$a = 67.4, b = 110.9,$ $c = 120.4$ $\alpha = \beta = \gamma = 90°$
V_M[d] (Å^3 Da^{-1})	2.00	4.23	2.00	1.99	2.01
Solvent (%)	38.4	70.9	38.5	38.1	38.9
Resolution (Å)	50–1.58 (1.61–1.58)	50–2.80 (2.85–2.80)	50–1.75 (1.81–1.75)	50–1.99 (2.02–1.99)	50–1.70 (1.73–1.70)
Measured refl.	1 502 448	845 333	865 507	787 079	1 319 072
Unique refl.	121 024 (5211)	46 836 (2173)	91 574 (9057)	61 848 (3022)	99 312 (4801)
Redundancy	12.4 (4.9)	18.0 (12.5)	9.5 (7.3)	12.7 (12.1)	13.3 (8.4)
Completeness (%)	98.4 (86.0)	97.1 (92.2)	100.0 (100.0)	99.7 (99.1)	99.8 (97.6)
$\langle I/\sigma \rangle$	21.4 (2.1)	34.1 (3.9)	27.5 (3.6)	34.1 (7.2)	30.0 (2.9)
R_{sym}[e] (%)	10.3 (44.2)	11.4 (71.8)	12.4 (62.3)	11.0 (53.0)	10.5 (54.2)

[a] Values in parenthesis are for the highest resolution shell.
[b] Contains citrate in the active site of subunit B.
[c] Also contains covalent Glu294 adducts: acetyl anhydride and CoA thioester.
[d] Matthews coefficient.
[e] $R_{sym} = \sum |I_h - \langle I_h \rangle| \,/\, \sum I_h$, where $\langle I_h \rangle$ is the average intensity over symmetry.

Table S9: Crystallographic refinement statistics for AarCH6.[a]

Ligands PDB entry	(none)[b] 4eu3	CoA 4eu4	CoA 4eu5	CoA, acetate[c] 4eu6	CoA, citrate 4eu7
Resolution (Å)	40.2–1.58 (1.64–1.58)	41.5–2.80 (2.90–2.80)	42.8–1.74 (1.81–1.74)	34.8–1.99 (2.02–1.99)	28.8–1.70 (1.76–1.70)
Refl. (working)	109 938	42 623	83 914	58 685	91 142
Refl. (test set)	5768	2273	4400	3092	4802
R_{cryst}[d] (%)	15.6 (25.8)	17.8 (28.7)	16.7 (21.8)	16.4 (16.5)	15.6 (22.3)
R_{free}[e] (%)	18.9 (29.8)	22.3 (35.9)	20.9 (28.3)	20.9 (24.3)	19.4 (26.7)
No. of atoms					
all atoms	9106	8179	8870	8488	9207
protein atoms	7817	7684	7789	7786	7843
ligand atoms	17	200	100	107	128
water atoms	1272	295	981	595	1236
Rms deviations					
bond lengths (Å)	0.006	0.008	0.006	0.007	0.006
bond angles (°)	1.07	1.20	1.06	1.05	1.04
Avg. B-factor (Å^2)					
protein atoms	12.6	49.7	17.0	22.4	17.0
ligand atoms	18.5	58.7	18.9	26.3	24.1
water atoms	24.8	45.0	25.9	27.9	29.4
Ramachandran plot (%)					
Most favored	97.0	92.5	97.0	96.8	96.6
Addl. allowed	2.9	6.9	2.7	2.8	3.2
Disallowed	0.1	0.6	0.3	0.4	0.2

[a] Values in parenthesis are for the highest resolution shell.
[b] Contains citrate in the active site of subunit B.
[c] Also contains covalent Glu294 adducts: acetyl anhydride and CoA thioester.
[d] $R_{\text{cryst}} = \sum |F_o - \langle F_c \rangle| \,/\, \sum F_o$, where the summation is over the data used for refinement.
[e] R_{free} is defined in the same way as R_{cryst} but was calculated using the 5% of the data that were excluded from refinement. With the exception of the 4eu8 and 4eua datasets, a consistent set of reflections was set aside for all datasets of the space group $P2_12_12_1$, including those datasets described in Table S11.

Table S10: Crystallographic data collection statistics for wild-type AarC and mutant AarCH6.[a]

	AarC	AarCH6-X				
X	(none)	S71A	R228E	R228E	E294A	E294A
Ligands	CoA, citrate	CoA, citrate	CoA	CoA	CoA	dethiaacetyl-CoA
PDB entry	4eud	4eu8	4eua	4eu9	4eub	4euc
Beamline	23-ID-B	21-ID-F	21-ID-D	21-ID-F	21-ID-F	21-ID-G
Wavelength (Å)	1.0332	0.97872	1.9075	0.97872	0.97872	0.97856
Space group	$P2_12_12_1$	$P2_12_12_1$	$P2_12_12_1$	$P2_12_12_1$	$P2_12_12_1$	$P2_12_12_1$
Cell dimen.[b] (Å)	$a = 67.7$	$a = 67.3$	$a = 67.4$	$a = 67.1$	$a = 67.4$	$a = 79.5$
	$b = 110.6$	$b = 109.7$	$b = 110.5$	$b = 110.1$	$b = 110.3$	$b = 104.1$
	$c = 119.9$	$c = 120.1$	$c = 119.2$	$c = 119.8$	$c = 120.2$	$c = 120.1$
V_M[c] (Å^3 Da^{-1})	2.05	1.99	1.99	1.98	2.00	2.33
Solvent (%)	40.1	38.0	37.9	38.1	38.6	44.8
Resolution (Å)	50–1.94	50–1.81	50–2.40	50–1.48	50–1.97	50–2.65
	(2.01–1.94)	(1.84–1.81)	(2.49–2.40)	(1.51–1.48)	(2.00–1.97)	(2.70–2.65)
Measured refl.	605 583	968 154	201 712	2 010 407	904 072	438 134
Unique refl.	64 164 (6136)	81 672 (4005)	34 893 (3477)	148 137 (7318)	63 807 (3167)	29 835 (1441)
Redundancy	9.4 (6.5)	11.9 (11.7)	5.8 (5.7)	13.6 (12.9)	14.2 (13.4)	14.7 (14.9)
Completeness (%)	97.3 (94.8)	100.0 (100.0)	98.2 (100.0)	99.9 (99.8)	100.0 (99.9)	100.0 (100.0)
$\langle I/\sigma \rangle$	20.0 (3.9)	40.3 (5.9)	54.6 (33.5)	38.4 (4.4)	28.4 (6.3)	33.9 (6.2)
R_{sym}[d] (%)	21.4 (60.0)	8.3 (48.2)	6.3 (10.9)	7.9 (57.4)	12.0 (49.1)	14.0 (75.4)

[a] Values in parenthesis are for the highest resolution shell.
[b] All are $\alpha = \beta = \gamma = 90°$.
[c] Matthews coefficient.
[d] $R_{sym} = \sum |I_h - \langle I_h \rangle| / \sum I_h$, where $\langle I_h \rangle$ is the average intensity over symmetry.

Table S11: Crystallographic refinement statistics for wild-type AarC and mutant AarCH6.[a]

	AarC	AarCH6-X				
X	(none)	S71A	R228E	R228E	E294A	E294A
Ligands	CoA, citrate	CoA	CoA	CoA	CoA	dethiaacetyl-CoA
PDB entry	4eud	4eu8	4eua	4eu9	4eub	4euc
Resolution (Å)	42.8–1.95	34.7–1.81	44.6–2.40	31.0–1.48	40.2–1.97	43.5–2.64
	(2.02–1.95)	(1.83–1.81)	(2.43–2.40)	(1.50–1.48)	(2.00–1.97)	(2.73–2.64)
Refl. (working)	57803	77516	62276	140548	60553	28286
Refl. (test set)	3021	4077	3330	7386	3179	1489
R_{cryst}[b] (%)	15.9 (17.8)	18.0 (24.0)	15.2 (15.3)	15.7 (19.1)	15.4 (18.2)	16.8 (22.2)
R_{free}[c] (%)	20.6 (26.0)	22.6 (29.6)	20.9 (23.6)	17.9 (22.1)	20.9 (26.4)	22.5 (29.7)
No. of atoms						
all atoms	8544	8513	8364	9290	8583	7987
protein atoms	7686	7724	7764	7862	7686	7676
ligand atoms	113	100	100	102	102	106
water atoms	745	689	500	1326	795	205
Rms deviations						
bond lengths (Å)	0.007	0.007	0.007	0.006	0.007	0.009
bond angles (°)	1.03	1.11	1.02	1.14	1.07	1.07
Avg. B-factor (Å^2)						
protein atoms	18.8	20.1	16.9	13.3	17.9	46.9
ligand atoms	29.1	27.1	31.3	20.0	14.3	43.9
water atoms	25.5	27.7	19.0	26.3	25.1	36.8
Ramachandran plot (%)						
Most favored	96.7	96.5	96.5	97.0	97.6	95.4
Addl. allowed	3.0	3.0	3.4	2.9	2.1	4.5
Disallowed	0.3	0.5	0.1	0.1	0.3	0.1

[a] Values in parenthesis are for the highest resolution shell.

[b] $R_{cryst} = \sum |F_o - \langle F_c \rangle| \,/\, \sum F_o$, where the summation is over the data used for refinement.

[c] R_{free} is defined in the same way as R_{cryst} but was calculated using the 5% of the data that were excluded from refinement. With the exception of the 4eu8 and 4eua datasets, a consistent set of reflections was set aside for all datasets of the space group $P2_12_12_1$, including those datasets described in Table S9.

Table S12: Model B: acetyl-CoA Michaelis complex.[a]

```
HETATM=8491==N1A=ACO=A3001======-7.059==13.267=-33.561==1.00=20.00===========N===
HETATM=8492==C2A=ACO=A3001======-5.857==13.789=-33.293==1.00=20.00===========C===
HETATM=8493==N3A=ACO=A3001======-5.579==14.335=-32.102==1.00=20.00===========N===
HETATM=8494==C4A=ACO=A3001======-6.512==14.366=-31.130==1.00=20.00===========C===
HETATM=8495==C5A=ACO=A3001======-7.767==13.824=-31.381==1.00=20.00===========C===
HETATM=8496==C6A=ACO=A3001======-8.023==13.268=-32.627==1.00=20.00===========C===
HETATM=8497==N6A=ACO=A3001======-9.322==12.689=-32.900==1.00=20.00===========N===
HETATM=8498==N7A=ACO=A3001======-8.502==13.980=-30.263==1.00=20.00===========N===
HETATM=8499==C8A=ACO=A3001======-7.749==14.595=-29.341==1.00=20.00===========C===
HETATM=8500==N9A=ACO=A3001======-6.545==14.831=-29.869==1.00=20.00===========N===
HETATM=8501==C1B=ACO=A3001======-5.440==15.427=-29.195==1.00=20.00===========C===
HETATM=8502==C2B=ACO=A3001======-5.618==16.897=-29.023==1.00=20.00===========C===
HETATM=8503==O2B=ACO=A3001======-5.215==17.576=-30.163==1.00=20.00===========O===
HETATM=8504==C3B=ACO=A3001======-4.741==17.145=-27.939==1.00=20.00===========C===
HETATM=8505==O3B=ACO=A3001======-3.400==17.061=-28.413==1.00=20.00===========O===
HETATM=8506==P3B=ACO=A3001======-2.336==18.282=-28.369==1.00=20.00===========P===
HETATM=8507==O7A=ACO=A3001======-1.834==18.440=-26.951==1.00=20.00===========O===
HETATM=8508==O8A=ACO=A3001======-1.182==17.913=-29.290==1.00=20.00===========O=1=
HETATM=8509==O9A=ACO=A3001======-2.956==19.597=-28.827==1.00=20.00===========O===
HETATM=8510==C4B=ACO=A3001======-4.934==15.989=-27.057==1.00=20.00===========C===
HETATM=8511==O4B=ACO=A3001======-5.357==14.939=-27.893==1.00=20.00===========O===
HETATM=8512==C5B=ACO=A3001======-5.994==16.253=-26.072==1.00=20.00===========C===
HETATM=8513==O5B=ACO=A3001======-7.217==16.708=-26.654==1.00=20.00===========O===
HETATM=8514==P1A=ACO=A3001======-8.443==17.215=-25.783==1.00=20.00===========P===
HETATM=8515==O1A=ACO=A3001======-9.546==17.587=-26.756==1.00=20.00===========O=1=
HETATM=8516==O2A=ACO=A3001======-8.046==18.403=-24.929==1.00=20.00===========O===
HETATM=8517==O3A=ACO=A3001======-9.020==16.035=-24.896==1.00=20.00===========O===
HETATM=8518==P2A=ACO=A3001======-8.607==15.587=-23.448==1.00=20.00===========P===
HETATM=8519==O4A=ACO=A3001======-7.928==16.651=-22.602==1.00=20.00===========O===
HETATM=8520==O5A=ACO=A3001======-9.889==15.097=-22.817==1.00=20.00===========O=1=
HETATM=8521==O6A=ACO=A3001======-7.601==14.391=-23.598==1.00=20.00===========O===
HETATM=8522==CBP=ACO=A3001======-6.959==12.090=-24.201==1.00=20.00===========C===
HETATM=8523==CCP=ACO=A3001======-7.907==13.313=-24.387==1.00=20.00===========C===
HETATM=8524==CDP=ACO=A3001======-5.596==12.477=-24.732==1.00=20.00===========C===
HETATM=8525==CEP=ACO=A3001======-7.504==10.861=-24.958==1.00=20.00===========C===
HETATM=8526==CAP=ACO=A3001======-6.819==11.782=-22.712==1.00=20.00===========C===
HETATM=8527==OAP=ACO=A3001======-8.086==11.594=-22.117==1.00=20.00===========O===
HETATM=8528==C9P=ACO=A3001======-5.955==10.563=-22.422==1.00=20.00===========C===
HETATM=8529==O9P=ACO=A3001======-4.733==10.569=-22.674==1.00=20.00===========O===
HETATM=8530==N8P=ACO=A3001======-6.627===9.328=-22.045==1.00=20.00===========N===
HETATM=8531==C7P=ACO=A3001======-5.862===8.156=-21.642==1.00=20.00===========C===
HETATM=8532==C6P=ACO=A3001======-5.732===7.926=-20.143==1.00=20.00===========C===
HETATM=8533==C5P=ACO=A3001======-7.061===7.778=-19.413==1.00=20.00===========C===
HETATM=8534==O5P=ACO=A3001======-8.123===7.842=-20.008==1.00=20.00===========O===
HETATM=8535==N4P=ACO=A3001======-7.029===7.404=-18.023==1.00=20.00===========N===
HETATM=8536==C3P=ACO=A3001======-8.274===7.270=-17.238==1.00=20.00===========C===
HETATM=8537==C2P=ACO=A3001======-7.957===7.278=-15.921==0.00==0.00===========C===
HETATM=8538==S1P=ACO=A3001======-6.698===8.488=-15.386==0.00==0.00===========S===
HETATM=8539==C===ACO=A3001======-5.220===7.850=-16.153==0.00==0.00===========C===
HETATM=8540==O===ACO=A3001======-5.243===6.790=-16.772==0.00==0.00===========O===
```

Table S12 – *Continued from previous page*

```
HETATM=8541==CH3=ACO=A3001======-3.945===8.612=-15.966==0.00==0.00==========C===
TER====8541======ACO=A3001=
CONECT=8491=8492=8496
CONECT=8492=8491=8493
CONECT=8493=8492=8494
CONECT=8494=8493=8495=8500
CONECT=8495=8494=8496=8498
CONECT=8496=8491=8495=8497
CONECT=8497=8496
CONECT=8498=8495=8499
CONECT=8499=8498=8500
CONECT=8500=8494=8499=8501
CONECT=8501=8500=8502=8511
CONECT=8502=8501=8503=8504
CONECT=8503=8502
CONECT=8504=8502=8505=8510
CONECT=8505=8504=8506
CONECT=8506=8505=8507=8508=8509
CONECT=8507=8506
CONECT=8508=8506
CONECT=8509=8506
CONECT=8510=8504=8511=8512
CONECT=8511=8501=8510
CONECT=8512=8510=8513
CONECT=8513=8512=8514
CONECT=8514=8513=8515=8516=8517
CONECT=8515=8514
CONECT=8516=8514
CONECT=8517=8514=8518
CONECT=8518=8517=8519=8520=8521
CONECT=8519=8518
CONECT=8520=8518
CONECT=8521=8518=8523
CONECT=8522=8523=8524=8525=8526
CONECT=8523=8521=8522
CONECT=8524=8522
CONECT=8525=8522
CONECT=8526=8522=8527=8528
CONECT=8527=8526
CONECT=8528=8526=8529=8530
CONECT=8529=8528
CONECT=8530=8528=8531
CONECT=8531=8530=8532
CONECT=8532=8531=8533
CONECT=8533=8532=8534=8535
CONECT=8534=8533
CONECT=8535=8533=8536
CONECT=8536=8535=8537
CONECT=8537=8536=8538
CONECT=8538=8537=8539
```

Table S12 – *Continued from previous page*

```
CONECT=8539=8538=8540=8541
CONECT=8540=8539
CONECT=8541=8539
END
```

[a] Adding these coordinates to PDB id 4eu6 will place modeled atoms in the active site of subunit A. COA A2598 and ACT A1428 should be deleted. Each "=" symbol should be replaced with a space.

Table S13: Model D1: acetate Michaelis complex.[a]

```
HETATM=8542==C===ACY=A3003======-3.849===7.872=-15.674==1.00=20.00==========C===
HETATM=8543==O===ACY=A3003======-3.792===7.459=-14.479==1.00=20.00==========O===
HETATM=8544==OXT=ACY=A3003======-4.454===7.387=-16.678==1.00=20.00==========O===
HETATM=8545==CH3=ACY=A3003======-3.104===9.159=-15.881==1.00=20.00==========C===
TER====8545======ACY=A3003=
HETATM=8616==C===ACY=B3003=====-18.430=-19.042=-24.149==0.00=20.00==========C===
HETATM=8617==O===ACY=B3003=====-18.813=-19.204=-22.953==0.00=20.00==========O===
HETATM=8618==OXT=ACY=B3003=====-17.614=-18.203=-24.639==0.00=20.00==========O===
HETATM=8619==CH3=ACY=B3003=====-19.028=-20.046=-25.092==0.00=20.00==========C===
TER====8619======ACY=B3003=
CONECT=8542=8543=8544=8545
CONECT=8543=8542
CONECT=8544=8542
CONECT=8545=8542
CONECT=8616=8617=8618=8619
CONECT=8617=8616
CONECT=8618=8616
CONECT=8619=8616
END
```

[a] Adding these coordinates to PDB id 4eu6 will place modeled atoms in the active site of subunits A and B. ACT A1428 should be deleted. Each "=" symbol should be replaced with a space. Subunit A allows comparisons with other models. Subunit B is the modeled Michaelis complex containing the glutamyl-CoA thioester.

Table S14: Model E: succinate Michaelis complex.[a]

```
HETATM=8546==C1==SIN=A3004======-3.994===7.459=-15.720==1.00=20.00==========C===
HETATM=8547==O1==SIN=A3004======-4.674===6.927=-16.664==1.00=20.00==========O===
HETATM=8548==O2==SIN=A3004======-4.089===7.274=-14.472==1.00=20.00==========O===
HETATM=8549==C2==SIN=A3004======-2.898===8.385=-16.152==1.00=20.00==========C===
HETATM=8550==C3==SIN=A3004======-2.177===9.019=-14.987==1.00=20.00==========C===
HETATM=8551==C4==SIN=A3004======-1.100==10.046=-15.271==1.00=20.00==========C===
HETATM=8552==O3==SIN=A3004======-1.405==11.105=-15.876==1.00=20.00==========O===
HETATM=8553==O4==SIN=A3004=======0.051===9.820=-14.772==1.00=20.00==========O===
TER====8553======SIN=A3004=
HETATM=8620==C1==SIN=B3004=====-18.300=-18.664=-23.966==0.00=20.00==========C===
HETATM=8621==O1==SIN=B3004=====-17.430=-17.815=-24.365==0.00=20.00==========O===
HETATM=8622==O2==SIN=B3004=====-18.538=-19.063=-22.789==0.00=20.00==========O===
HETATM=8623==C2==SIN=B3004=====-19.198=-19.220=-25.029==0.00=20.00==========C===
HETATM=8624==C3==SIN=B3004=====-20.159=-20.256=-24.497==0.00=20.00==========C===
HETATM=8625==C4==SIN=B3004=====-21.071=-20.970=-25.473==0.00=20.00==========C===
HETATM=8626==O3==SIN=B3004=====-20.566=-21.665=-26.391==0.00=20.00==========O===
HETATM=8627==O4==SIN=B3004=====-22.322=-20.911=-25.235==0.00=20.00==========O===
TER====8627======SIN=B3004=
CONECT=8546=8547=8548=8549
CONECT=8547=8546
CONECT=8548=8546
CONECT=8549=8546=8550
CONECT=8550=8549=8551
CONECT=8551====8=8550=8552
CONECT=8552=8551
CONECT====8=8551
CONECT=8620=8621=8622=8623
CONECT=8621=8620
CONECT=8622=8620
CONECT=8623=8620=8624
CONECT=8624=8623=8625
CONECT=8625=8624=8626=8627
CONECT=8626=8625
CONECT=8627=8625
END
```

[a] Adding these coordinates to PDB id 4eu6 will place modeled atoms in the active site of subunits A and B. ACT A1428 should be deleted. Each "=" symbol should be replaced with a space. Subunit A allows comparisons with other models. Subunit B is the modeled Michaelis complex containing the glutamyl-CoA thioester.

Table S15: Model F: glutamylsuccinyl anhydride adduct.[a]

```
HETATM=8554==C4==SIN=A3005======-4.440===7.703=-15.499==1.00=20.00==========C===
HETATM=8555==O3==SIN=A3005======-4.952===7.094=-16.431==1.00=20.00==========O===
HETATM=8556==C3==SIN=A3005======-3.256===8.603=-15.762==1.00=20.00==========C===
HETATM=8557==C2==SIN=A3005======-1.900===8.290=-15.309==1.00=20.00==========C===
HETATM=8558==C1==SIN=A3005======-1.135===9.588=-15.536==1.00=20.00==========C===
HETATM=8559==O1==SIN=A3005======-1.674==10.540=-16.157==1.00=20.00==========O===
HETATM=8560==O2==SIN=A3005=======0.015===9.648=-15.012==1.00=20.00==========O===
TER====8560======SIN=A3005=
CONECT=8554=8555=8556
CONECT=8555=8554
CONECT=8556=8554=8557
CONECT=8557=8556=8558
CONECT=8558=8557=8559=8560
CONECT=8559=8558
CONECT=8560=8558
END
```

[a] Adding these coordinates to PDB id 4eu6 will place modeled atoms in the active site of subunit A. ACT A1428 should be deleted. Each "=" symbol should be replaced with a space. Atoms C4, O3, and C3 have not been modeled, but are renumbered atoms from ACT A1428.

Table S16: Model G: succinyl-CoA Michaelis complex.[a]

```
HETATM=8561==C8==SCA=A3006======-7.746==14.579=-29.340==1.00=20.00===========C===
HETATM=8562==N9==SCA=A3006======-6.542==14.815=-29.868==1.00=20.00===========N===
HETATM=8563==C4==SCA=A3006======-6.509==14.350=-31.129==1.00=20.00===========C===
HETATM=8564==C5==SCA=A3006======-7.764==13.808=-31.380==1.00=20.00===========C===
HETATM=8565==N7==SCA=A3006======-8.499==13.964=-30.262==1.00=20.00===========N===
HETATM=8566==N3==SCA=A3006======-5.576==14.319=-32.101==1.00=20.00===========N===
HETATM=8567==C2==SCA=A3006======-5.854==13.773=-33.292==1.00=20.00===========C===
HETATM=8568==N1==SCA=A3006======-7.056==13.251=-33.560==1.00=20.00===========N===
HETATM=8569==C6==SCA=A3006======-8.020==13.252=-32.626==1.00=20.00===========C===
HETATM=8570==N6==SCA=A3006======-9.319==12.673=-32.899==1.00=20.00===========N===
HETATM=8571==C1'=SCA=A3006======-5.437==15.411=-29.194==1.00=20.00===========C===
HETATM=8572==C2'=SCA=A3006======-5.615==16.881=-29.022==1.00=20.00===========C===
HETATM=8573==O2'=SCA=A3006======-5.212==17.560=-30.162==1.00=20.00===========O===
HETATM=8574==C3'=SCA=A3006======-4.738==17.129=-27.938==1.00=20.00===========C===
HETATM=8575==O3'=SCA=A3006======-3.397==17.045=-28.412==1.00=20.00===========O===
HETATM=8576==C4'=SCA=A3006======-4.931==15.973=-27.056==1.00=20.00===========C===
HETATM=8577==O4'=SCA=A3006======-5.354==14.923=-27.892==1.00=20.00===========O===
HETATM=8578==C5'=SCA=A3006======-5.991==16.237=-26.071==1.00=20.00===========C===
HETATM=8579==O5'=SCA=A3006======-7.214==16.692=-26.653==1.00=20.00===========O===
HETATM=8580==P1==SCA=A3006======-8.440==17.199=-25.782==1.00=20.00===========P===
HETATM=8581==O11=SCA=A3006======-9.543==17.571=-26.755==1.00=20.00===========O=1=
HETATM=8582==O12=SCA=A3006======-8.043==18.387=-24.928==1.00=20.00===========O===
HETATM=8583==O6==SCA=A3006======-9.017==16.019=-24.895==1.00=20.00===========O===
HETATM=8584==P2==SCA=A3006======-8.604==15.571=-23.447==1.00=20.00===========P===
HETATM=8585==O21=SCA=A3006======-9.886==15.081=-22.816==1.00=20.00===========O=1=
HETATM=8586==O22=SCA=A3006======-7.925==16.635=-22.601==1.00=20.00===========O===
HETATM=8587==O7==SCA=A3006======-7.598==14.375=-23.597==1.00=20.00===========O===
HETATM=8588==CPB=SCA=A3006======-7.904==13.297=-24.386==1.00=20.00===========C===
HETATM=8589==CPA=SCA=A3006======-6.956==12.074=-24.200==1.00=20.00===========C===
HETATM=8590==CP7=SCA=A3006======-6.816==11.766=-22.711==1.00=20.00===========C===
HETATM=8591==CP9=SCA=A3006======-7.501==10.845=-24.957==1.00=20.00===========C===
HETATM=8592==CP8=SCA=A3006======-5.593==12.461=-24.731==1.00=20.00===========C===
HETATM=8593==OP3=SCA=A3006======-8.083==11.578=-22.116==1.00=20.00===========O===
HETATM=8594==NP2=SCA=A3006======-6.624===9.312=-22.044==1.00=20.00===========N===
HETATM=8595==CP5=SCA=A3006======-5.859===8.140=-21.641==1.00=20.00===========C===
HETATM=8596==CP4=SCA=A3006======-5.729===7.910=-20.142==1.00=20.00===========C===
HETATM=8597==CP3=SCA=A3006======-7.058===7.762=-19.412==1.00=20.00===========C===
HETATM=8598==CP6=SCA=A3006======-5.952==10.547=-22.421==1.00=20.00===========C===
HETATM=8599==OP2=SCA=A3006======-4.730==10.553=-22.673==1.00=20.00===========O===
HETATM=8600==OP1=SCA=A3006======-8.120===7.826=-20.007==1.00=20.00===========O===
HETATM=8601==NP1=SCA=A3006======-7.026===7.388=-18.022==1.00=20.00===========N===
HETATM=8602==CP2=SCA=A3006======-8.271===7.254=-17.237==1.00=20.00===========C===
HETATM=8603==CP1=SCA=A3006======-7.977===7.167=-15.963==0.00==0.00===========C===
HETATM=8604==P3==SCA=A3006======-2.333==18.266=-28.368==1.00=20.00===========P===
HETATM=8605==O31=SCA=A3006======-1.831==18.424=-26.950==1.00=20.00===========O===
HETATM=8606==O32=SCA=A3006======-1.179==17.897=-29.289==1.00=20.00===========O=1=
HETATM=8607==O33=SCA=A3006======-2.953==19.581=-28.826==1.00=20.00===========O===
HETATM=8608==S===SCA=A3006======-6.819===8.400=-15.311==0.00==0.00===========S===
HETATM=8609==CS1=SCA=A3006======-5.243===7.889=-16.050==0.00==0.00===========C===
```

Table S16 – *Continued from previous page*

```
HETATM=8610==OS1=SCA=A3006======-5.172===6.838=-16.676==0.00==0.00==========O===
HETATM=8611==CS2=SCA=A3006======-4.100===8.845=-15.836==0.00==0.00==========C===
HETATM=8612==CS3=SCA=A3006======-2.669===8.346=-15.696==0.00==0.00==========C===
HETATM=8613==CS4=SCA=A3006======-1.728===9.564=-15.805==0.00==0.00==========C===
HETATM=8614==OS4=SCA=A3006======-0.535===9.441=-15.389==0.00==0.00==========O===
HETATM=8615==OS5=SCA=A3006======-2.226==10.608=-16.310==0.00==0.00==========O===
TER====8615======SCA=A3006=
CONECT=8561=8562=8565
CONECT=8562=8561=8563=8571
CONECT=8563=8562=8564=8566
CONECT=8564=8563=8565=8569
CONECT=8565=8561=8564
CONECT=8566=8563=8567
CONECT=8567=8566=8568
CONECT=8568=8567=8569
CONECT=8569=8564=8568=8570
CONECT=8570=8569
CONECT=8571=8562=8572=8577
CONECT=8572=8571=8573=8574
CONECT=8573=8572
CONECT=8574=8572=8575=8576
CONECT=8575=8574=8604
CONECT=8576=8574=8577=8578
CONECT=8577=8571=8576
CONECT=8578=8576=8579
CONECT=8579=8578=8580
CONECT=8580=8579=8581=8582=8583
CONECT=8581=8580
CONECT=8582=8580
CONECT=8583=8580=8584
CONECT=8584=8583=8585=8586=8587
CONECT=8585=8584
CONECT=8586=8584
CONECT=8587=8584=8588
CONECT=8588=8587=8589
CONECT=8589=8588=8590=8591=8592
CONECT=8590=8589=8593=8598
CONECT=8591=8589
CONECT=8592=8589
CONECT=8593=8590
CONECT=8594=8595=8598
CONECT=8595=8594=8596
CONECT=8596=8595=8597
CONECT=8597=8596=8600=8601
CONECT=8598=8590=8594=8599
CONECT=8599=8598
CONECT=8600=8597
CONECT=8601=8597=8602
CONECT=8602=8601=8603
```

Table S16 – *Continued from previous page*

```
CONECT=8603=8602=8608
CONECT=8604=8575=8605=8606=8607
CONECT=8605=8604
CONECT=8606=8604
CONECT=8607=8604
CONECT=8608=8603=8609
CONECT=8609=8608=8610=8611
CONECT=8610=8609
CONECT=8611=8609=8612
CONECT=8612=8611=8613
CONECT=8613=8612=8614=8615
CONECT=8614=8613
CONECT=8615=8613
END
```

[a] Adding these coordinates to PDB id 4eu6 will place modeled atoms in the active site of subunit A. COA A2598 and ACT A1428 should be deleted. Each "=" symbol should be replaced with a space.

Table S17: Conserved catalytic residues and catalytic water in phylogenetically diverse class I CoA-transferases.[a]

Accession	PDB id	Z (identity)					
SCACT (succinyl-CoA:acetate CoA-transferase) group							
B3EY95	4eu7	–	Val270	Glu294	Asn347	Gly388	HOH517
Q9HTC2	2g39	56 (48%)	Ile264	Glu288	Asn341	Gly382	HOH947
Q7MVN7	2nvv	53 (48%)	Val259	Glu284	Asn337	Gly378	–[b]
4HBCT (4-hydroxybutyrate CoA-transferase) group							
Q8EG98	2oas	37 (26%)	Ile211	Glu233	Asn290	Gly331	–[b]
Q9RM86	3gk7[c]	36 (24%)	Ile216	Glu238	Asn295	Gly336	HOH486
Q9ZC36	3qli	35 (25%)	Val227	Glu249	Asn306	Gly347	HOH466
Other CoA-transferases							
Q29551	3oxo[d]	22 (18%)	Ile284	Glu305	Gln99	Gly386	–[b]
Q8X5X6	2ahv[e]	21 (16%)	Val309	Glu333	Gln118	Gly401	HOH2682
P76458 (α)[f]	1k6d[g]	16 (α: 18%)	–	–	Glnα100	–	–[b]
Q59111 (α)[f]	1poi	15 (α: 14%)	Thrβ31	Gluβ54	Glnα103	Glyβ137	HOHβ270
Q59112 (β)[f]		9.6 (β: 18%)					

[a] Conserved or equivalent residues in structurally related class I CoA-transferases were identified by a structure-based alignment (DALI server) using AarCH6 as the query structure. Comparisons are with subunit A except where noted. Spatially conserved waters were identified in manual alignments.
[b] A water was not modeled at this position in 1k6d (missing β subunit), 2nvv (2.7 Å dataset), 2oas (2.4 Å), or 3oxo (2.3 Å).
[c] PDB id 3gk7 and PDB id 3qdq (Figures 7, S13, and S14) are the same protein.
[d] Comparison is with chain C.
[e] Comparison is with chain D.
[f] The α and β subunits of the heterotetrameric CoA-transferases correspond to the N- and C-terminal domains of the homodimeric CoA-transferases.
[g] The structure contains only the α subunit.

Table S18: Selected class I CoA-transferases that have been crystallographically or functionally characterized.

Accession	PDB id	Functional assignment (gene product)	Source	Ref(s)
SCACT (succinyl-CoA:acetate CoA-transferase) group[a]				
B3EY95	4eu7	SCACT (AarC)	*Acetobacter aceti*	S9, this work
F5TSW6[b]	–	propionate CoA-transferase[c]	*Propionibacterium acnes*	S11
P38946	–	putative SCACT (Cat1)	*Clostridium kluyveri*	S12
Q9HTC2	2g39	putative SCACT	*Pseudomonas aeruginosa*	–
Q7MVN7	2nvv	putative SCACT	*Porphyromonas gingivalis*	–
P52043	–	propionyl-CoA:succinate CoA-transferase (YgfH)	*Escherichia coli*	S13
4HBCT (4-hydroxybutyrate CoA-transferase) group[d]				
Q8EG98	2oas	4HBCT	*Shewanella oneidensis*	–
Q9RM86	3gk7	4HBCT	*Clostridium aminobutyricum*	S3,S14,S15
Q9ZC36	3qli	butyryl- or propionyl-CoA transferase (RipA)	*Yersinia pestis*	S16
Other CoA-transferases[e]				
Q29551	3oxo	succinyl-CoA:3-oxoacid CoA-tranferase (SCOT)	*Sus scrofa*	S17
Q8X5X6	2ahv	short-chain-fatty-acid CoA-transferase (YdiF)	*Escherichia coli* O157:H7	S18
P76458 (α)[f]	1k6d (α)	acetate CoA-transferase (ACT)	*Escherichia coli*	S19
P76459 (β)[f]	–			
Q59111 (α)[f]	1poi ($\alpha\beta$)	glutaconate CoA-transferase (GCT)	*Acidaminococcus fermentans*	S20
Q59112 (β)[f]				

[a] TIGR03458 sequence family.

[b] BLASTP searches identified only one close homologue of AarC ($E = 0$) in every sequenced *Propionibacterium* genome. Most *Propionibacterium* genomes also contain a 4HBCT homologue that is less similar to AarC ($E \sim 10^{-14}$).

[c] CoA-transferase activity was measured in crude mixtures. This enzyme functions equally well with propionyl-CoA or acetyl-CoA when succinate is the CoA-acceptor.

[d] TIGR03948 sequence family.

[e] Includes representative class I CoA-transferases from other groups within the superfamily.[S21]

[f] The α and β subunits of the heterotetrameric CoA-transferases correspond to the N- and C-terminal domains of homodimeric CoA-transferases.

Table S19: Full kinetic data for selected AarCH6 mutants.[a]

parameter	wild-type[b]	S71A[c]	R228E[d]	N347A[e]	E435D
acetate					
k_{cat} (s^{-1})	280 ± 40	4.85 ± 0.07	3.4 ± 0.1[f]	12.2 ± 0.2	370 ± 50
K_m (mM)	70 ± 20	167 ± 6	6 ± 1[f]	78 ± 5	110 ± 30
K_i (mM)	1600 ± 800	NA[g]	NA	NA	2000 ± 2000
k_{cat}/K_m ($M^{-1}\,s^{-1}$)	$(4 \pm 1) \times 10^3$	$(2.9 \pm 0.1) \times 10^1$	$(6 \pm 1) \times 10^2$	$(1.6 \pm 0.1) \times 10^2$	$(3 \pm 1) \times 10^3$
succinyl-CoA					
k_{cat} (s^{-1})	201 ± 8	6.2 ± 0.6	16.0 ± 0.4	10.8 ± 0.4	340 ± 10
K_m (μM)	22 ± 4	90 ± 20	122 ± 9	28 ± 4	40 ± 5
k_{cat}/K_m ($M^{-1}\,s^{-1}$)	$(9 \pm 2) \times 10^6$	$(7 \pm 2) \times 10^4$	$(1.3 \pm 0.1) \times 10^5$	$(3.9 \pm 0.6) \times 10^5$	$(9 \pm 1) \times 10^6$
succinate					
k_{cat} (s^{-1})	71 ± 2	6.2 ± 0.1	800 ± 500	2.07 ± 0.02	153 ± 2
K_m (mM)	0.9 ± 0.1	21 ± 2	3000 ± 2000	0.76 ± 0.03	2.1 ± 0.1
k_{cat}/K_m ($M^{-1}\,s^{-1}$)	$(7.9 \pm 0.9) \times 10^4$	$(3.0 \pm 0.3) \times 10^2$	$(3 \pm 3) \times 10^2$	$(2.7 \pm 0.1) \times 10^3$	$(7.3 \pm 0.4) \times 10^4$
acetyl-CoA					
k_{cat} (s^{-1})	75 ± 2	40 ± 20	105 ± 3	1.92 ± 0.06	129 ± 3
K_m (μM)	22 ± 2	500 ± 300	45 ± 5	2.8 ± 0.4	25 ± 3
K_i (μM)	NA	70 ± 40	NA	NA	NA
k_{cat}/K_m ($M^{-1}\,s^{-1}$)	$(3.4 \pm 0.3) \times 10^6$	$(8 \pm 6) \times 10^4$	$(2.3 \pm 0.3) \times 10^6$	$(7 \pm 1) \times 10^5$	$(5.2 \pm 0.6) \times 10^6$
K_{eq}[h]	0.13	0.08	0.1	0.033	0.071

[a] SCACT activities were measured using LCF/LCR assays. Saturation experiments were performed in duplicate for mutant enzymes.
[b] From Ref. S9.
[c] Initial kinetic analysis revealed a nonlinear decrease in specific activity at low enzyme concentrations. LCF and LCR assay methods were altered to obtain consistent initial velocities.
[d] Higher fixed substrate concentrations were used: acetate saturation, 500 μM succinyl-CoA; succinyl-CoA saturation, 750 mM acetate; acetyl-CoA saturation, 550 mM succinate.
[e] In succinate saturation experiments, the fixed concentration of acetyl-CoA was 100 μM
[f] Based on the empirical fitting model described in Figure S18.
[g] NA, not applicable.
[h] Computed using k_{cat}/K_m values as (succinyl-CoA × acetate)/(succinate × acetyl-CoA).[S22]

Supporting Figures

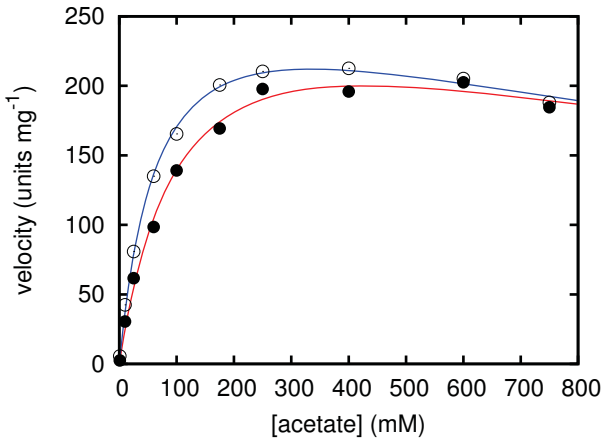

Figure S1: Acetate saturation curves for AarC (filled circles) and AarCH6 (open circles). The solid lines are fits to the experimental data assuming substrate inhibition. Parameters for AarC and AarCH6 are given in the main text and Table S19, respectively.

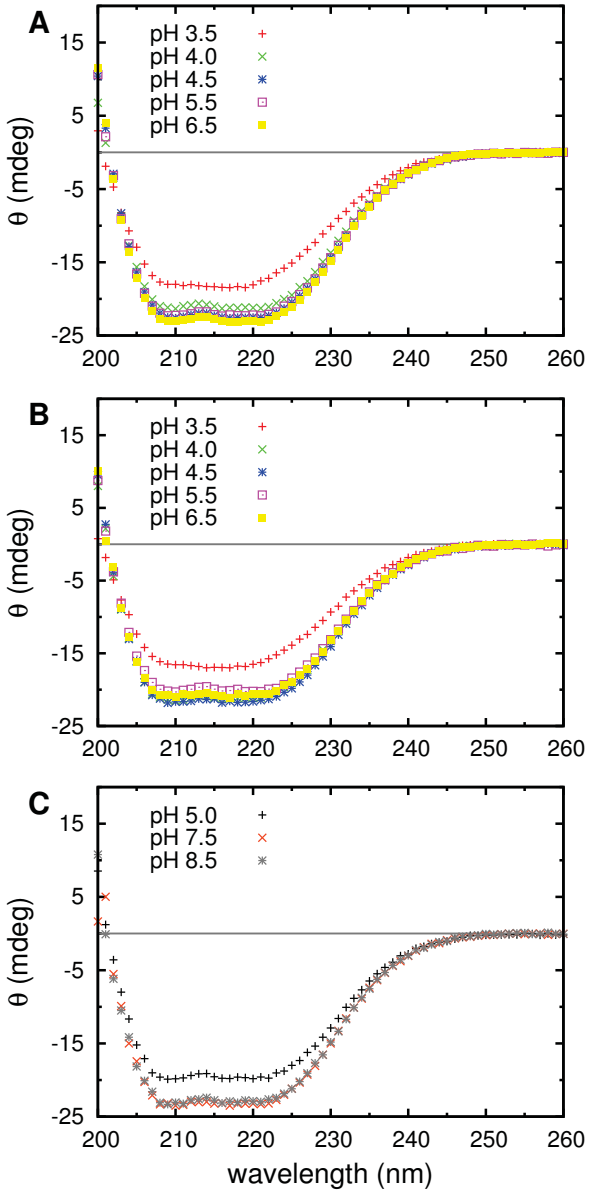

Figure S2: Circular dichroism spectra acquired at various pH values. (A) AarC spectra. (B) AarCH6 spectra. (C) Additional AarCH6 spectra.

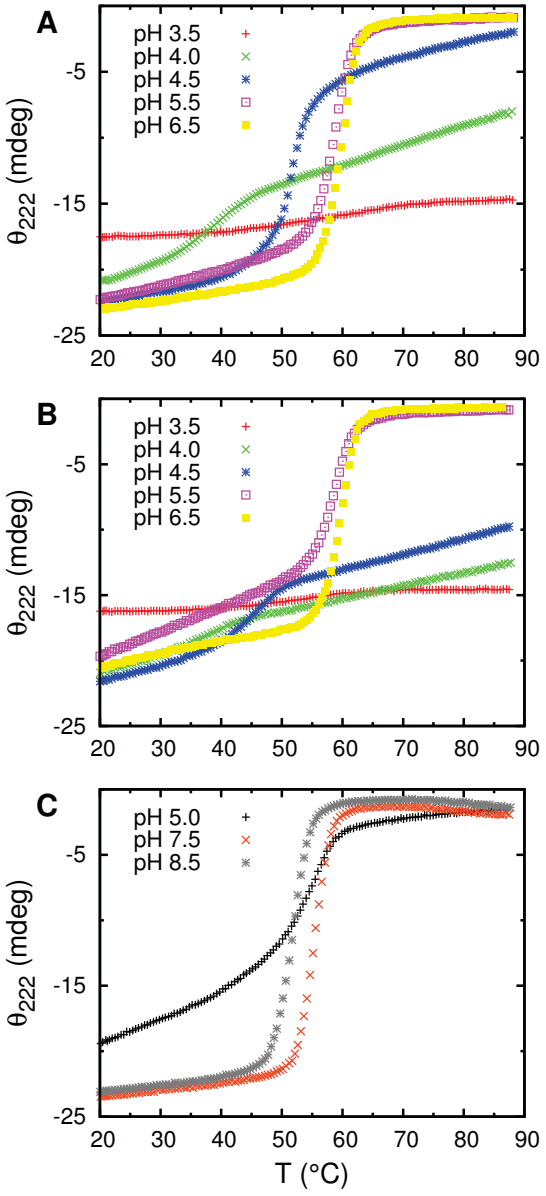

Figure S3: Melting profiles obtained at various pH values. Circular dichroism signal was monitored at 222 nm. (A) AarC melts. (B) AarCH6 melts. (C) Additional AarCH6 melts.

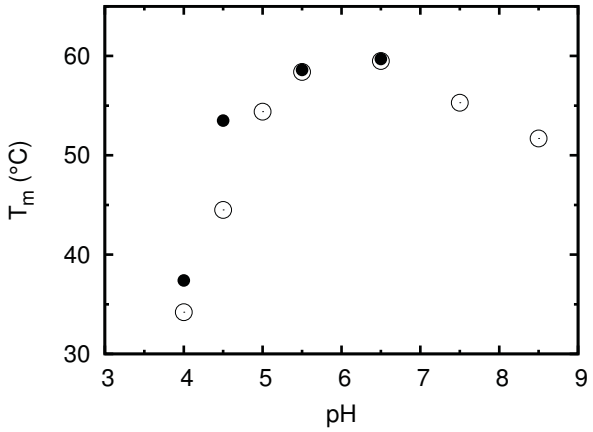

Figure S4: Thermal denaturation of AarC (filled circles) and AarCH6 (larger open circles) from melting profiles (Figure S3) as a function of pH. At low pH, the hexahistidine tag appears to destabilize AarCH6 relative to AarC.

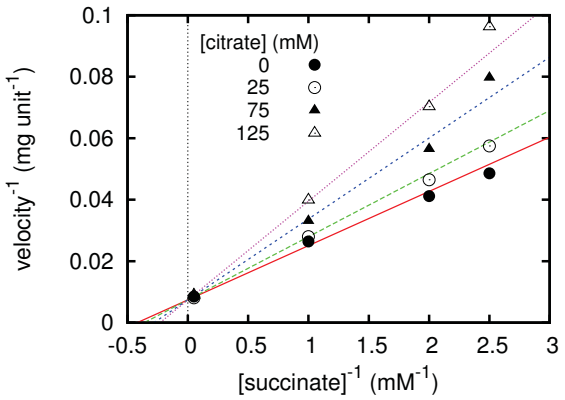

Figure S5: Citrate-dependent inhibition of AarCH6. Citrate is a competitive inhibitor versus succinate. LCR velocity data were fit to Equation 2. Fitted values are $V = 135 \pm 2$ units mg^{-1}, $K_m^{\text{succinate}} = 2.4 \pm 0.1$ mM, and $K_i = 150 \pm 20$ mM. The line shown for each citrate concentration was computed from a global fit of the data obtained at all citrate concentrations.

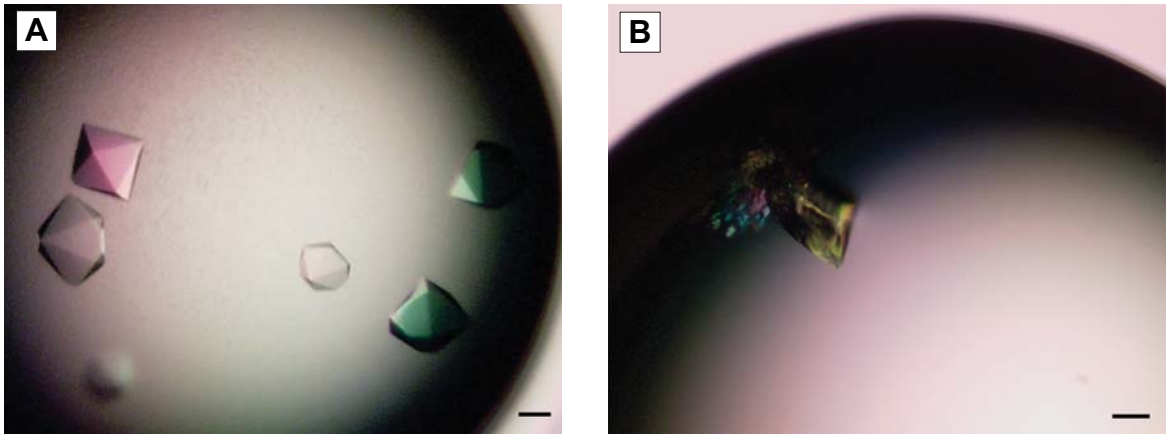

Figure S6: AarCH6 crystals. (A) Hexagonal crystals grown in ammonium sulfate. (B) Orthorhombic crystals grown in sodium citrate. Black bars represent 0.1 mm.

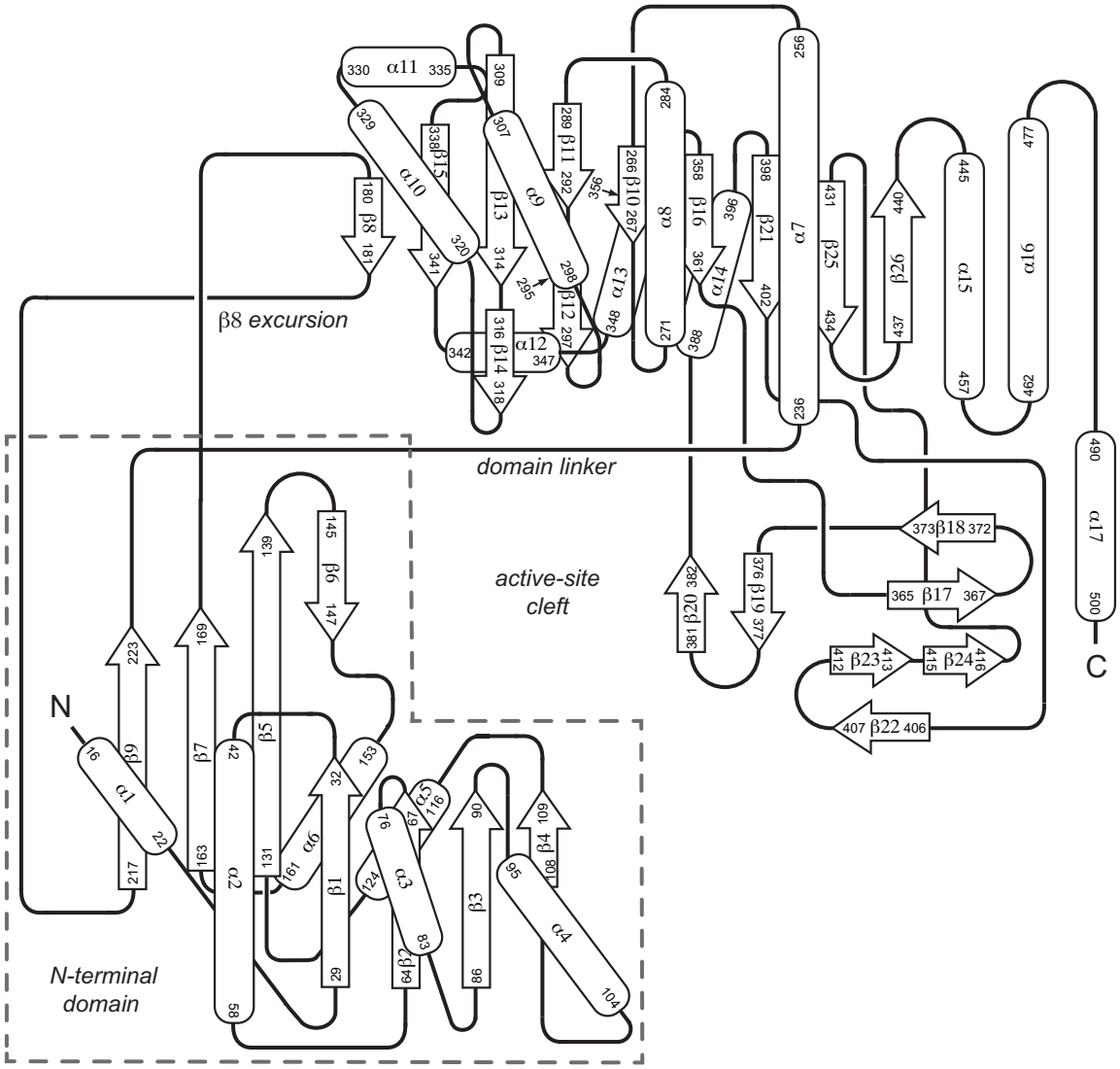

Figure S7: AarC(H6) topology diagram. Each subunit is composed of distinct N- and C-terminal domains, displaying open α/β folds. The domains are joined by a flexible domain linker that spans a deep active-site cleft. The N-terminal domain possesses a three layer architecture: a core seven-strand parallel β-sheet (β9, β7, β5, β1, β2, β3, β4) with a single antiparallel edge (β6) is sandwiched between four surface-exposed α-helices ($\alpha 1 - \alpha 4$) and two partly buried α-helices (α5 and α6) at the subunit interface. The C-terminal domain is similarly arranged: a core eight-strand parallel β-sheet (β8, β15, β13, β11, β10, β16, β21, β25) with a single antiparallel edge (β26) is sandwiched between five surface-exposed α-helices ($\alpha 7 - \alpha 11$) and three buried α-helices (α12 – α14) at the subunit interface. A two-strand parallel β-sheet (β12 and β14) oriented perpendicularly to the main sheet is part of the domain interface. The C-terminal domain is additionally composed of two two-strand antiparallel β-sheets (β19/β20 and β22/β23), a three-strand mixed β-sheet (β17, β18, and β24), and three flanking α-helices ($\alpha 15 - \alpha 17$). All 3_{10}-helices are omitted.

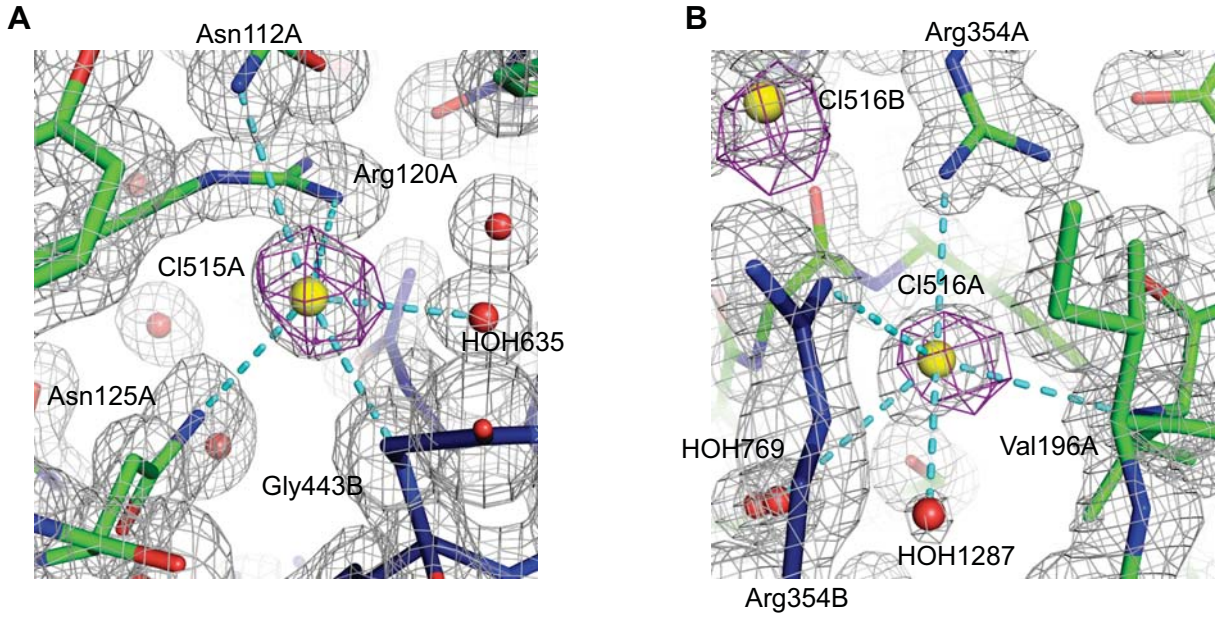

Figure S8: Chloride ions at the monomer-monomer interface in the AarCH6$-$R$_{228}$E$\cdot$CoA complex (PDB id 4eu9). Four chloride ions (yellow spheres) are associated with buried and otherwise uncompensated arginine residues at the subunit interface (subunit A, green; subunit B, blue). The σA-weighted $2mF_o - DF_c$ map (gray, PDB id 4eu9) is contoured at 1.5σ. The NCS-averaged, σA-weighted anomalous map (purple, PDB id 4eua) is contoured at 2.8σ. Neither map is carved in the region shown. Coulombic interactions are indicated (cyan dotted lines).

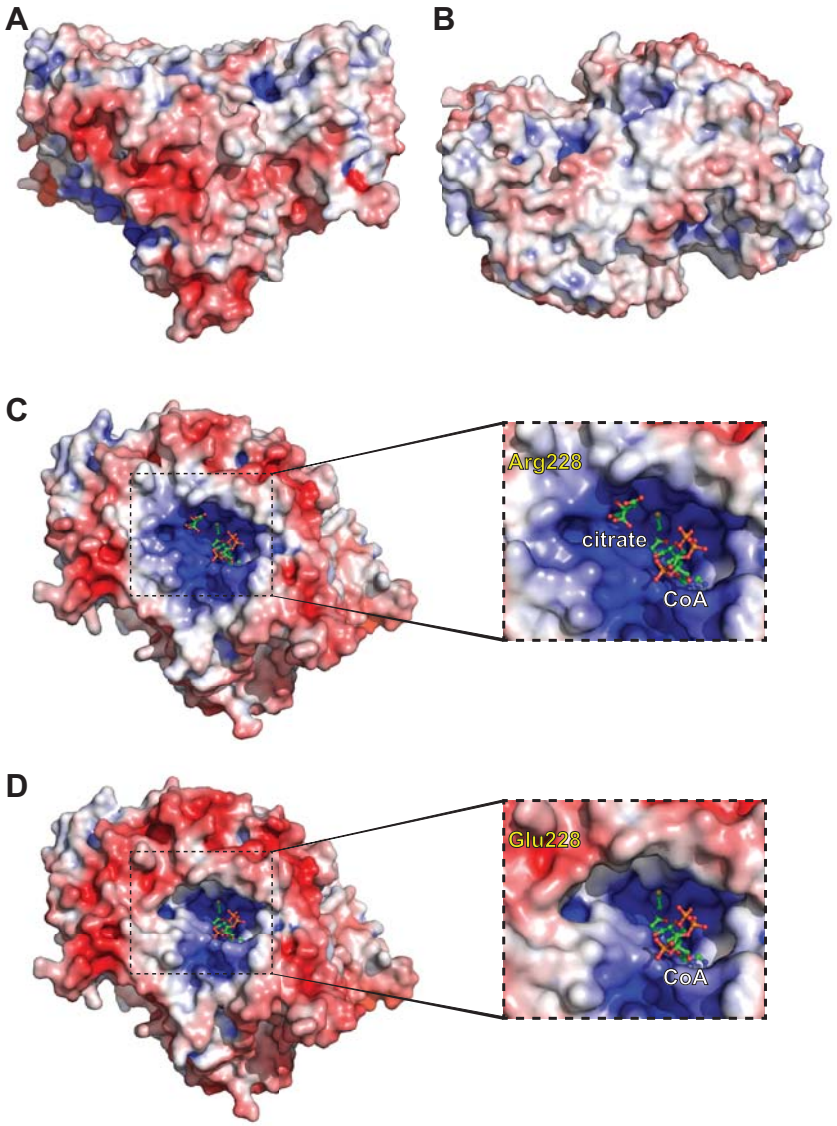

Figure S9: Electrostatic surface representation of AarCH6 and AarCH6-R228E. (A) AarCH6 · CoA · citrate complex (PDB id 4eu7), oriented with the pseudo-twofold axis vertical and in the plane of the page. (B) AarCH6 · CoA · citrate complex oriented with the pseudo-twofold axis emerging perpendicularly from the page. (C) AarCH6 · CoA · citrate complex oriented with the active site of subunit A at the center. (D) AarCH6-R228E · CoA complex (PDB id 4eu9) oriented as in panel C. The surfaces are colored red for negatively charged areas and blue for positively charged areas. The saturation of the colors is proportional to the degree of electrostatic charge from $-7kT/e$ to $+7kT/e$. CoA and citrate are depicted in stick representation.

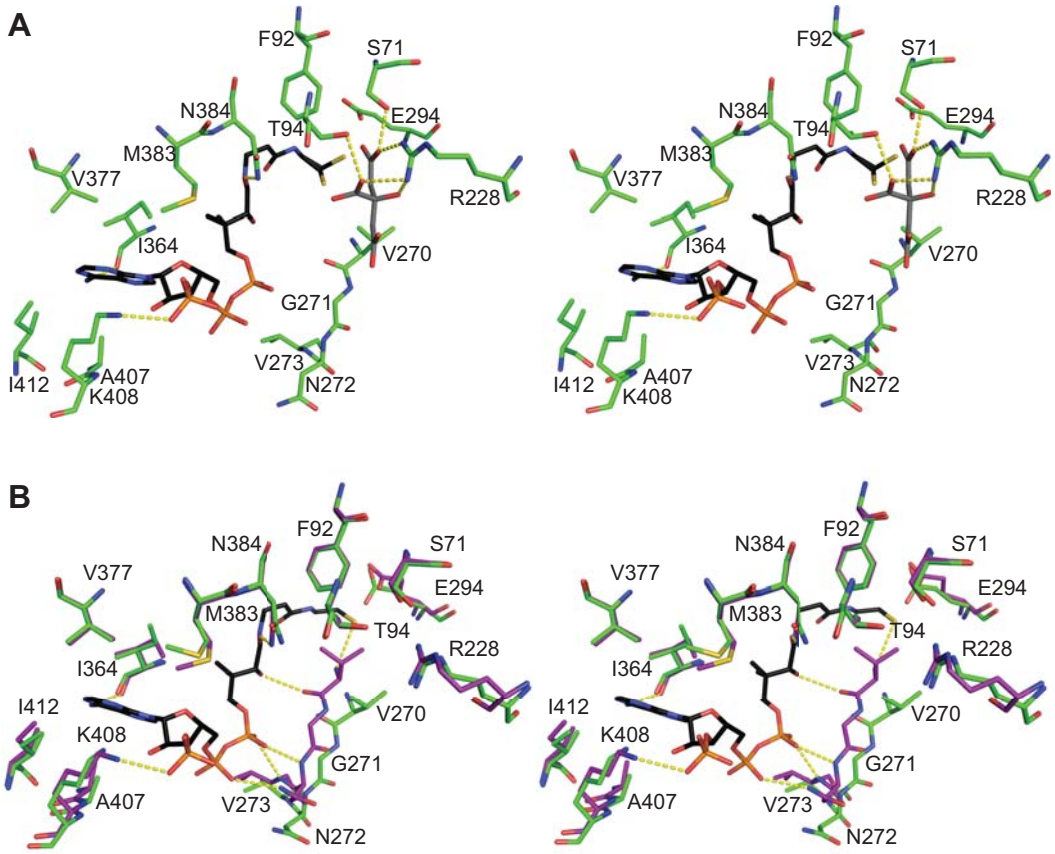

Figure S10: Protein conformation and ligand binding sites. (A) Divergent stereodiagram showing the binding sites for CoA and citrate near the active site glutamate Glu294 in the AarCH6 · CoA · citrate complex (PDB id 4eu7). Citrate interacts with Ser71, Thr94, and Arg228. The citrate pro-*S* carboxylate (in front of V270) interacts only with solvent and has higher temperature factors than the rest of the ligand. CoA interacts with Ile364, Asn384, and Lys408. All other hydrogen-bonding interactions with CoA are mediated by solvent (not shown). The subterminal methylene C9″ and terminal thiol of CoA were modeled in two alternate conformations. (B) Divergent stereodiagram showing how constriction of the active-site cleft maximizes electrostatic and hydrogen-bonding interactions (yellow dotted lines) with CoA. Residues in the open conformation are colored green (PDB id 4eu3), residues in the mostly closed conformation are colored purple (PDB id 4eu5), and CoA is colored black. In the mostly open conformation (PDB id 4eu7), only three direct hydrogen bonds are present between CoA and the protein (Ile364, Asn384, and Lys408), while all other hydrogen bonds are water mediated (Supporting Information, Figure S10A). In the mostly and fully closed conformations (PDB ids 4eu5 and 4eub; Supporting Information, Figure S10B), five additional hydrogen bonds are present between CoA and a mobile loop (Val270) and the N-terminus of helix α8 (Asn272 and Val273). In both panels, hydrogen bonds are indicated with yellow dotted lines.

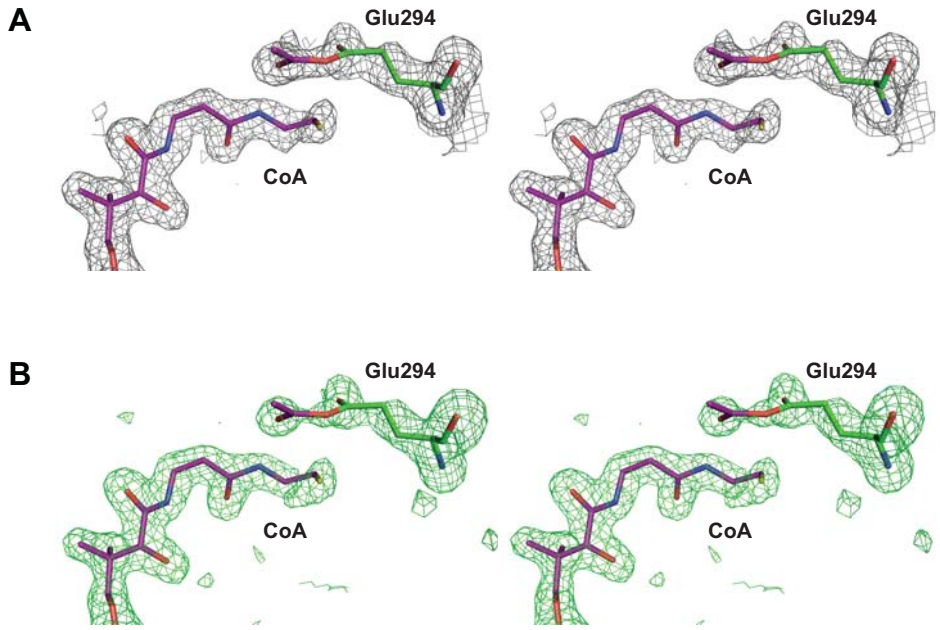

Figure S11: Electron density corresponding to the acetylglutamyl anhydride adduct and the CoA thiolate intermediate (PDB id 4eu6, subunit A). (A) Divergent stereodiagram showing a σA-weighted $2mF_o - DF_c$ omit map contoured at 0.9σ and carved with a 2 Å radius. (B) Divergent stereodiagram showing a σA-weighted $mF_o - DF_c$ omit map contoured at 3.0σ and carved with a 5 Å radius. Neither map displays significant electron density consistent with acetyl-CoA or the glutamyl-CoA thioester adduct.

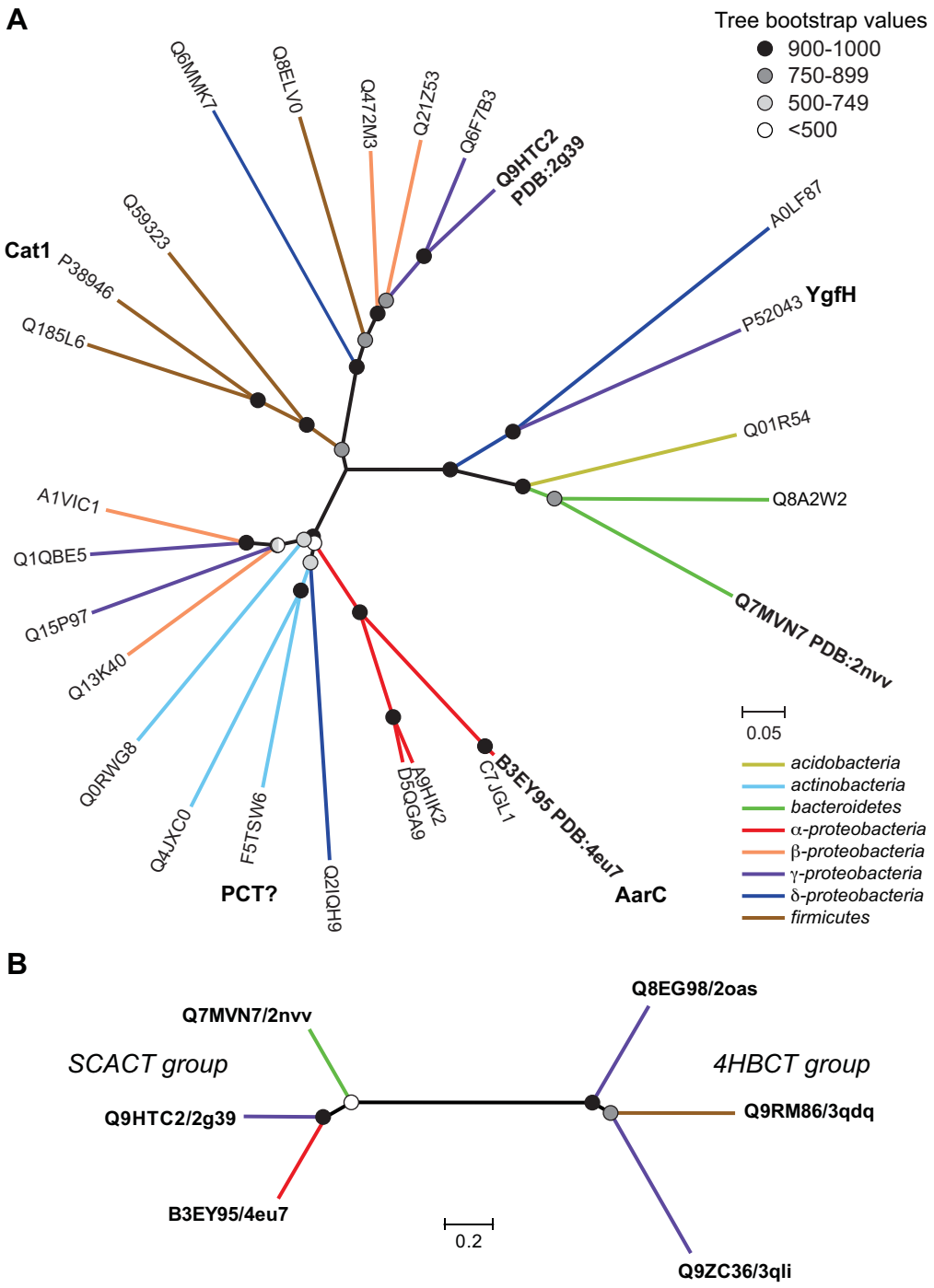

Figure S12: Unrooted radial cladograms. (A) SCACT group (TIGR03458 family), based on structure-based sequence alignment SBSA3. (B) Structurally characterized representatives of the SCACT and 4HBCT groups, based on structure-based sequence alignment SBSA6 (Figure S13). UniProt id numbers are given for each taxon. In panel A, taxa in bold letters have been crystallographically characterized (representative PDB ids are given), two overlapped junctions are at the root of the Q13K40 branch, and gene names are given for the four proteins that have been biochemically characterized, including PCT, a putative *Propionibacterium* propionate CoA-transferase (Table S18). Branches are color-coded by bacterial taxonomic group. Tree bootstrap value ranges (of 1000 NJ replicates) are indicated with circles at each junction.

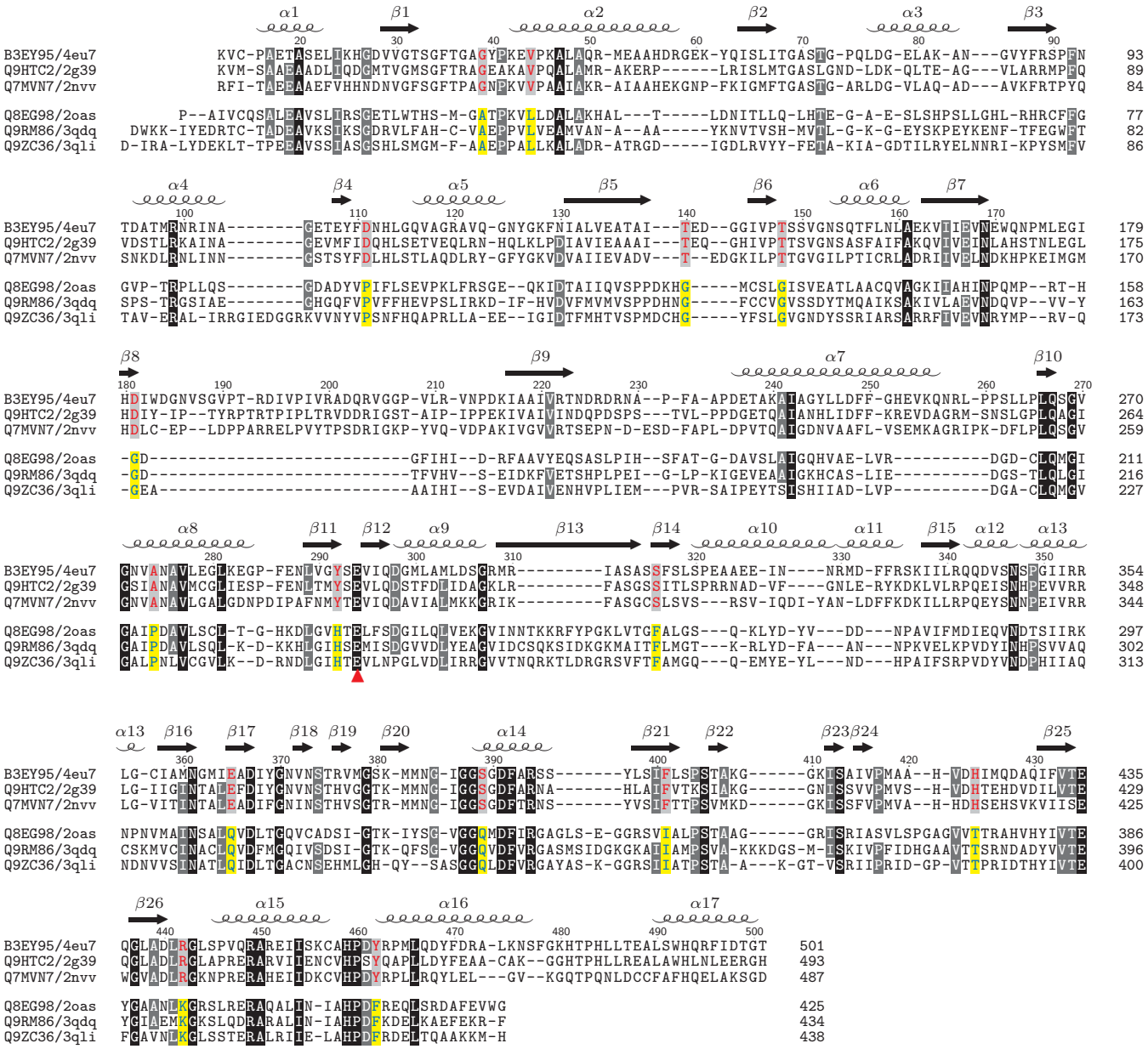

Figure S13: Full structure-based sequence alignment of representatives of the SCACT (top three) and 4HBCT (bottom three) groups. The catalytic glutamate is highlighted with a red arrow. The 4HBCT group lacks the $\beta 8$ excursion (Figure S7) present in the SCACT group. Together with its pseudosymmetric partner, the AarC $\beta 8$ excursion covers a helical region, located near the pseudo-twofold axis on the face of the dimer opposite the active-site cleft, that would be solvent-accessible in the 4HBCT group. Globally conserved residues are shown with a black background/white letters at invariant positions and gray background/white letters at highly conserved positions. Strictly *differentially* conserved residues are shown with a gray background/red letters (SCACT group) or a yellow background/blue letters (4HBCT group). A subset of this sequence alignment is shown as Figure 7B.

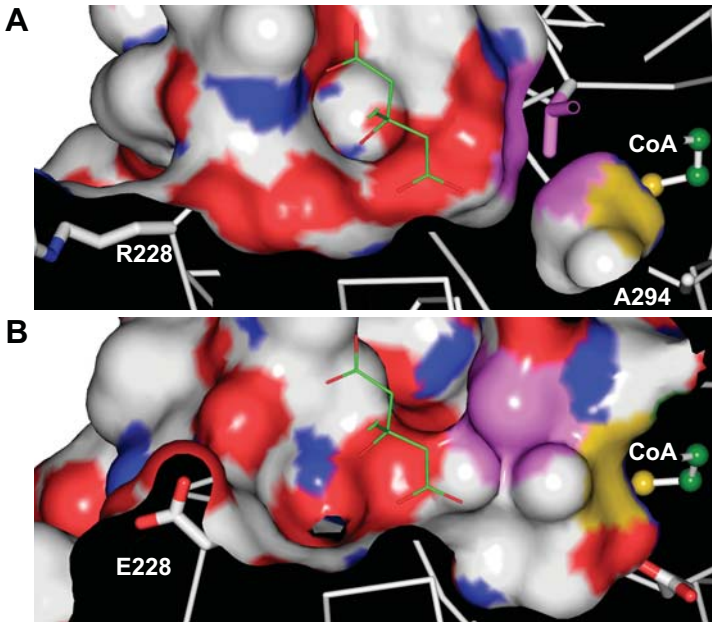

Figure S14: Regulation of carboxylate access to the active site glutamate. Panels were prepared as described for Figure 9 but are shown with an extension to the left to depict the outward orientation of the residue at position 228. Citrate from the AarCH6 · CoA · citrate complex (PDB id 4eu7), superposed using full-length subunits, is shown as thin green lines; the central carboxylate is partially clipped by the near plane. (A) The AarCH6-E294A · CoA complex (PDB id 4eub, subunit B) adopts the fully closed conformation in which Val270 (purple) prevents carboxylate or bulk solvent access to the catalytic pocket. The mutant enlarges the pocket volume somewhat. (B) The AarCH6-R228E · CoA complex (PDB id 4eu9, subunit B) adopts the mostly open conformation. The charge-reversed side chain of Glu228 is in an outward orientation that is usually associated with the closed conformation.

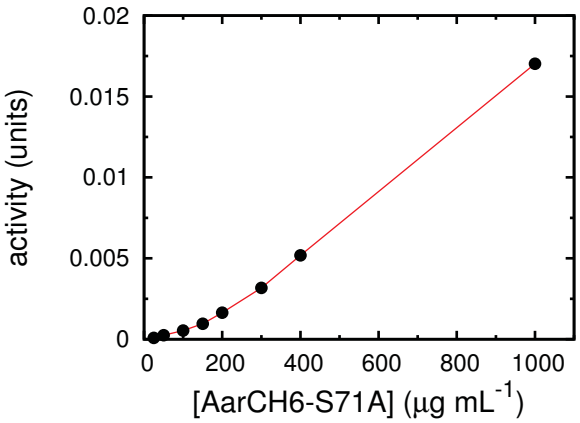

Figure S15: Activity versus AarCH6-S71A concentration. Initial kinetic characterization of AarCH6-S71A revealed a nonlinear decrease in specific activity at low enzyme concentrations. Reaction mixtures contained 50 – 5000 ng AarCH6-S71A (0.18 – 18 μM subunit concentration). Dimer dissociation into less active monomers might account for this phenomenon, which was not observed in any other form of AarC(H6). Gel-filtration analysis of AarCH6-S71A at 4 °C and a much higher initial concentration (6 $mg\,mL^{-1}$) showed a single peak at an elution volume most consistent with a dimeric solution state (91 kDa observed, 112 kDa expected; K. L. Sullivan, data not shown).

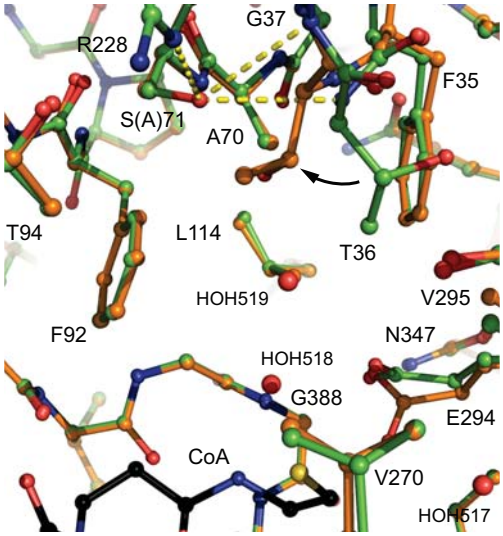

Figure S16: Partial collapse of the succinate binding pocket in AarCH6-S71A. Propionate was used in place of succinate to assess whether the diminished activity of AarCH6-S71A (Table S19) was due to deletion of the C4 carboxylate – Ser71 hydrogen-bonding interaction. Acetyl-CoA dependent conversion of propionate to propionyl-CoA by AarCH6-S71A (k_{cat} = 8 ± 1 s^{-1}, K_m = 900 ± 200 mM, and k_{cat}/K_m = 8 ± 2 M^{-1} s^{-1}) was slower than that of wt AarCH6 (Table S4) by about the same factor as the acetyl-CoA dependent conversion of succinate to succinyl-CoA. It therefore appears unlikely that the catalytic impairment is due solely to the removal of a single enzyme-substrate hydrogen-bonding interaction. Without the three structural hydrogen-bonding interactions (yellow dotted lines) formed between the side chain of Ser71, the side chain of Arg228, and the backbone nitrogens of Thr36 and Gly37, the loop connecting $\beta 1$ and $\alpha 2$ shifted. In the resulting conformation, the side chain of Thr36 blocks a large portion of the succinate binding pocket. This rearrangement may account for the large loss of catalytic activity. Additionally, Arg228 was extruded from the active site in both the open and the closed conformations (PDB id 4eu8 subunit A and subunit B, respectively), effectively eliminating the auxiliary carboxylate binding site. CoA and all waters are omitted from the AarCH6 model (green, PDB id 4eu5). CoA (black) and two placeholder waters are included from the AarCH6-S71A model (orange, PDB id 4eu8). HOH520 (Figure 6) was displaced by Thr36.

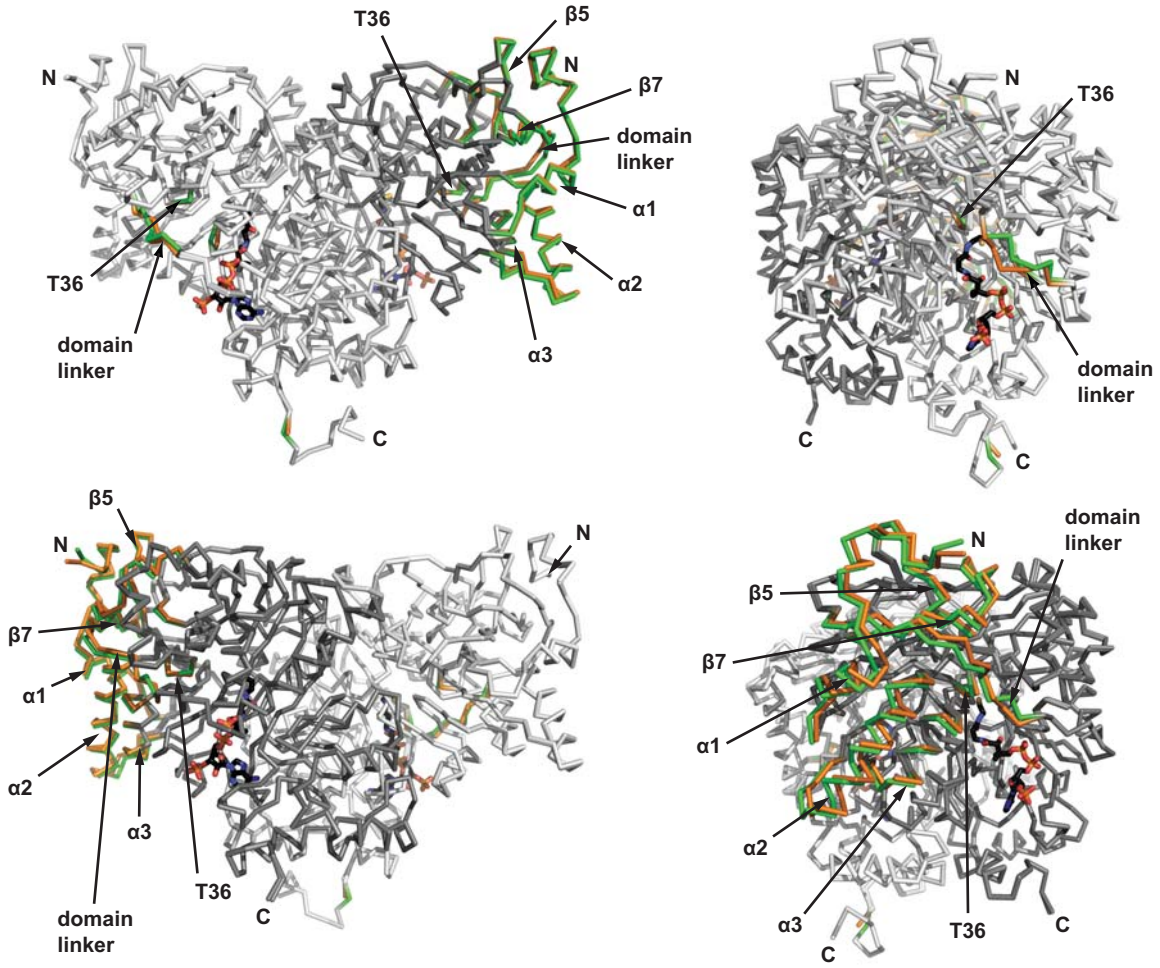

Figure S17: Conformational motions in AarCH6-S71A. Superposed views of AarCH6 and AarCH6-S71A are shown in each panel. In the open conformation (light gray, subunit A), AarCH6-S71A (PDB id 4eu8) displays only minor local structural rearrangements relative to AarCH6 (PDB id 4eu5). In the closed conformation (dark gray, subunit B), however, AarCH6-S71A exhibits widespread, coordinated conformational shifts in the N-terminal domain, the domain linker, and the loops flanking strand $\beta 8$. In both conformations, the loss of the hydrogen-bonding interaction between Ser71 and Arg228 allowed the side chain of Arg228 to be pulled out of the active-site cleft. Dynamic regions (Cα r.m.s.d. $\geq$0.75 Å) are colored green (AarCH6) and orange (AarCH6-S71A). CoA from the AarCH6-S71A complex is colored black.

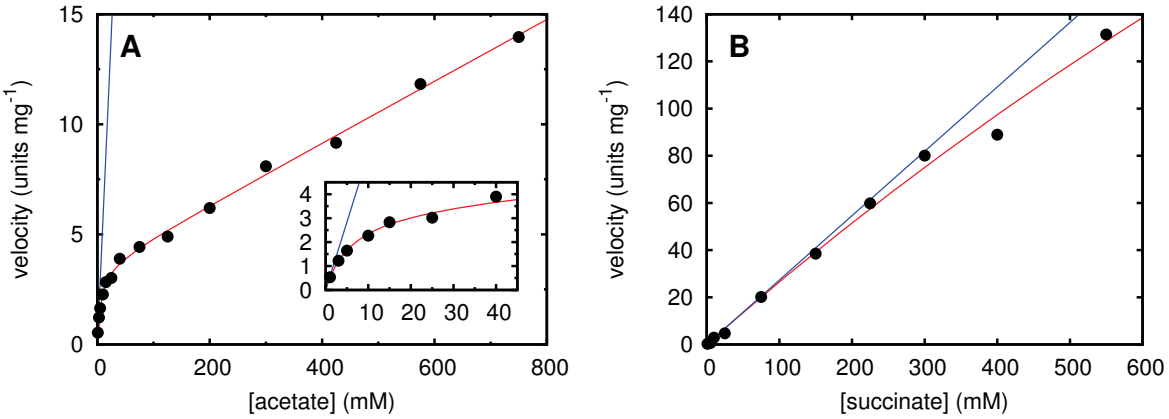

Figure S18: Velocity versus substrate concentration curves for AarCH6-R228E. Both curves are consistent with incomplete substrate saturation. (A) Acetate saturation curve, assayed at 0.5 mM succinyl-CoA. The red line is a fit of the data to an equation that assumes parallel Michaelis-Menten and first-order kinetic processes, $v = S(k_{\mathrm{cat}}E/(K_{\mathrm{m}}+S)+k)$. The fit is empirical, and no mechanism by which this might occur is assumed. The blue line is a plot of $S \times k_{\mathrm{cat}}/K_{\mathrm{m}}$, using the values obtained by fitting the empirical equation. *Inset*, Expansion of the lower concentration range. (B) Succinate saturation curve, assayed at 1 mM acetyl-CoA. The lines are fits obtained as in panel A. A full set of kinetic parameters obtained by this analysis is given in Table S19. Estimated V/K_{m} values for acyl-CoA substrates are given in Table 3.

References

(S1) Holm, L., and Rosenström, P. (2010) Dali server: conservation mapping in 3D. *Nucleic Acids Res. 38*, W545–W549.

(S2) Lee, J., and Kim, S. H. (2009) *PDB Editor*: a user-friendly Java-based Protein Data Bank file editor with a GUI. *Acta Crystallogr. D Biol. Crystallogr. 65*, 399–402.

(S3) Macieira, S., Zhang, J., Velarde, M., Buckel, W., and Messerschmidt, A. (2009) Crystal structure of 4-hydroxybutyrate CoA-transferase from *Clostridium aminobutyricum*. *Biol. Chem. 390*, 1251–1263.

(S4) Meng, E. C., Pettersen, E. F., Couch, G. S., Huang, C. C., and Ferrin, T. E. (2006) Tools for integrated sequence-structure analysis with UCSF Chimera. *BMC Bioinformatics 7*, 339.

(S5) Waterhouse, A. M., Procter, J. B., Martin, D. M. A., Clamp, M., and Barton, G. J. (2009) Jalview Version 2–a multiple sequence alignment editor and analysis workbench. *Bioinformatics 25*, 1189–1191.

(S6) Marchler-Bauer, A., and Bryant, S. H. (2004) CD-Search: protein domain annotations on the fly. *Nucleic Acids Res. 32*, W327–W331.

(S7) Tamura, K., Peterson, D., Peterson, N., Stecher, G., Nei, M., and Kumar, S. (2011) MEGA5: molecular evolutionary genetics analysis using maximum likelihood, evolutionary distance, and maximum parsimony methods. *Mol. Biol. Evol. 28*, 2731–2739.

(S8) Brandt, B. W., Feenstra, K. A., and Heringa, J. (2010) Multi-Harmony: detecting functional specificity from sequence alignment. *Nucleic Acids Res. 38*, W35–W40.

(S9) Mullins, E. A., Francois, J. A., and Kappock, T. J. (2008) A specialized citric acid cycle requiring succinyl-coenzyme A (CoA):acetate CoA-transferase (AarC) confers acetic acid resistance on the acidophile *Acetobacter aceti*. *J. Bacteriol. 190*, 4933–4940.

(S10) Nath, A., and Atkins, W. M. (2008) A quantitative index of substrate promiscuity. *Biochemistry 47*, 157–166.

(S11) Allen, S. H. G., Kellermeyer, R. W., Stjernholm, R. L., and Wood, H. G. (1964) Purification and properties of enzymes involved in the propionic acid fermentation. *J. Bacteriol. 87*, 171–187.

(S12) Söhling, B., and Gottschalk, G. (1996) Molecular analysis of the anaerobic succinate degradation pathway in *Clostridium kluyveri*. *J. Bacteriol. 178*, 871–880.

(S13) Haller, T., Buckel, T., Rétey, J., and Gerlt, J. A. (2000) Discovering new enzymes and metabolic pathways: conversion of succinate to propionate by *Escherichia coli*. *Biochemistry 39*, 4622–4629.

(S14) Scherf, U., and Buckel, W. (1991) Purification and properties of 4-hydroxybutyrate coenzyme A transferase from *Clostridium aminobutyricum*. *Appl. Environ. Microbiol. 57*, 2699–2702.

(S15) Macieira, S., Zhang, J., Buckel, W., and Messerschmidt, A. (2012) Crystal structure of the complex between 4-hydroxybutyrate CoA-transferase from *Clostridium aminobutyricum* and CoA. *Arch. Microbiol. 194*, 157–166.

(S16) Torres, R., Swift, R. V., Chim, N., Wheatley, N., Lan, B., Atwood, B. R., Pujol, C., Sankaran, B., Bliska, J. B., Amaro, R. E., and Goulding, C. W. (2011) Biochemical, structural and molecular dynamics analyses of the potential virulence factor RipA from *Yersinia pestis*. *PLoS One 6*, e25084.

(S17) Fraser, M. E., Hayakawa, K., and Brown, W. D. (2010) Catalytic role of the conformational change in succinyl-CoA:3-oxoacid CoA transferase on binding CoA. *Biochemistry 49*, 10319–10328.

(S18) Rangarajan, E. S., Li, Y., Ajamian, E., Iannuzzi, P., Kernaghan, S. D., Fraser, M. E., Cygler, M., and Matte, A. (2005) Crystallographic trapping of the glutamyl-CoA thioester intermediate of family I CoA transferases. *J. Biol. Chem. 280*, 42919–42928.

(S19) Korolev, S., Koroleva, O., Petterson, K., Gu, M., Collart, F., Dementieva, I., and Joachimiak, A. (2002) Autotracing of *Escherichia coli* acetate CoA-transferase α-subunit structure using 3.4 Å MAD and 1.9 Å native data. *Acta Crystallogr. D Biol. Crystallogr. 58*, 2116–2121.

(S20) Jacob, U., Mack, M., Clausen, T., Huber, R., Buckel, W., and Messerschmidt, A. (1997) Glutaconate CoA-transferase from *Acidaminococcus fermentans*: the crystal structure reveals homology with other CoA-transferases. *Structure 5*, 415–426.

(S21) Anantharaman, V. and Aravind, L. (2006) Diversification of catalytic activities and ligand interactions in the protein fold shared by the sugar isomerases, eIF2B, DeoR transcription factors, acyl-CoA transferases and methenyltetrahydrofolate synthetase. *J. Mol. Biol. 356*, 823–842.

(S22) Cleland, W. W. (1982) An analysis of Haldane relationships. *Methods Enzymol. 87*, 366–369.